https://doi.org/10.5194/egusphere-2026-4372
Preprint. Discussion started: 11 August 2026

Nitrogen fixation and atmospheric deposition influences on Mediterranean surface and intermediate water nutrient dynamics

Adam Francis[1,2*], Robyn E. Tuerena[2], Raja S. Ganeshram[1], Markus Ankele[3], Alex R. Baker[4], Kirstin Dähnke[3], Sarah E. Reynolds[5], Ulrike Baranowski[1], Claire Mahaffey[6]

[1]School of Geosciences, University of Edinburgh, Edinburgh, EH9 3FE, UK
[2]Scottish Association for Marine Science; Dunstaffnage, Oban, PA37 1QA, UK
[3]Institute of Carbon Cycles, Helmholtz Centre Hereon, Geesthacht 21502, Germany
[4]Centre for Ocean and Atmospheric Sciences, School of Environmental Sciences, University of East Anglia, Norwich, NR4 7TJ, UK
[5]Faculty of Science and Health, School of Environment and Life Sciences, University of Portsmouth, PO1 2UP, UK
[6]Earth, Ocean and Ecological Sciences, University of Liverpool, L69 3BX, UK

**Correspondence to*: Adam Francis (adam.francis@ed.ac.uk)

Abstract

The Mediterranean Sea is an oligotrophic basin characterised by anti-estuarine circulation and low productivity. In comparison to the global average, nutrients in the upper water column have high nitrate: phosphate ratios (or N*, nitrate minus phosphate x 16), suggested to arise from high external nutrient inputs. Modified Atlantic Water (MAW) enters with a low inorganic/organic nitrogen ratio, becomes saltier and denser moving eastwards, sinks to form Levantine Intermediate Water (LIW) ultimately feeding the Mediterranean Overflow Water (MOW), supplying nutrients to the Atlantic. This study employed stoichiometric and isotopic analyses of nitrate, dissolved organic nitrogen (DON), and particulate nitrogen to assess the roles of atmospheric deposition and nitrogen fixation on nutrient dynamics within MAW and LIW formation regions.

In the western basin, atmospheric deposition, primarily from anthropogenic sources, dominates nitrogen inputs, maintaining a high N:P ratio (N*) and low $\delta^{15}N$ (~3.5‰) in MAW. Moving eastward, anthropogenic nitrogen inputs decline, lowering the atmospheric N:P contribution, allowing dust-derived phosphorus to be increasingly important and potentially stimulating nitrogen fixation. This further decreases $\delta^{15}N$ (< 3‰) while altering MAW nutrient stoichiometry (lower N* and nutrient concentrations, higher organic contributions), passing these into initial LIW properties. During LIW formation, dissolved organic phosphorus (DOP) concentration decreased, suggesting DOP hydrolysis via high alkaline phosphatase activity could support nitrogen fixation along with a dust-derived nutrient source. This could

https://doi.org/10.5194/egusphere-2026-4372
Preprint. Discussion started: 11 August 2026

contribute 54.94 ± 29.03 Gg N of new nitrogen, alongside direct atmospheric nitrogen inputs (7.4 - 37.2 Gg N). These new nitrogen additions are transferred to depth, forming the source composition of the LIW and influencing the properties of subsequent water masses formed further along the LIW pathway. At the basin scale, the LIW nitrogen content is largely determined by Atlantic DON, modified by changes in nitrogen inputs from atmospheric nitrogen deposition and nitrogen fixation to the surface water, controlled by phosphorus availability.

1 Introduction

The Mediterranean Sea is an oligotrophic inland sea characterised by low biological productivity, despite receiving significant external nutrient inputs. Subsurface waters have high nitrogen (N) to phosphorus (P) (N:P) ratios exceeding global ocean Redfield ratios (Garcia et al., 2006). An anti-estuarine circulation driven by excess evaporation over precipitation contributes to intermediate and deep-water formation (Bethoux, 1980; Krom et al., 2010; Millot and Taupier-Letage, 2005) influencing nutrient distributions and processing.

Atlantic inflow through the Strait of Gibraltar forms Modified Atlantic Water (MAW), which is low in inorganic nitrogen (nitrate) (< 4μM) and phosphorus (phosphate) (<0.2 μM) but richer in dissolved organic nitrogen (DON) (> 4 μM) and phosphorus (DOP) (> 0.2μM) (Powley et al., 2017b). MAW travels eastward, increasing in salinity and density until sinking to form Levantine Intermediate Water (LIW) in winter convection events mainly around the Rhodes Gyre (Fach et al., 2021; Ozsoy et al., 1981). The LIW is the Mediterranean's main intermediate water mass, and this formation site is where currents start to turn west and are subject to inputs from the Black Sea and Aegean. The LIW returns westwards across the Mediterranean below the surface MAW but mixes with this MAW in key regions during its transport to form deep waters until being exported back into the Atlantic. This exported water has altered biogeochemical properties, such as elevated inorganic nutrient concentrations relative to the initial inflow (Powley et al., 2017b). The LIW is pivotal for Mediterranean circulation as it facilitates the exchange of physical and biogeochemical properties between surface, intermediate and deep-water masses whilst retaining much of its MAW-derived source signature (Fach et al., 2021).

https://doi.org/10.5194/egusphere-2026-4372
Preprint. Discussion started: 11 August 2026

The Mediterranean basins differ biogeochemically, with the western basin having almost double the nutrient concentrations of the eastern basin (Moutin and Raimbault, 2002; Pujo-Pay et al., 2011), resulting in 2.5 - 3.3 times higher primary production (Berman-Frank and Rahav, 2012). N:P ratios are elevated in the east (26 - 30:1) relative to the west (20 - 23:1) (Béthoux et al., 1998; Krom et al., 1991; Moutin and Raimbault, 2002) for both inorganic (nitrate: phosphate) and organic (DON: DOP) ratios (Banoub and Williams, 1972; Krom et al., 2005; Pujo-Pay et al., 2011), indicating overall phosphorus limitation in the Mediterranean but especially in the ultraoligotrophic eastern basin (Krom et al., 2005). Nitrogen isotope ratios of nitrate ($\delta^{15}N$-NO_3) in the intermediate and deep water are lower than the global ocean (2 - 3‰ vs 4.8‰) and increase westward (following LIW flow) along with increasing nutrient concentrations (Emeis et al., 2010; Pantoja et al., 2002). Elevated Mediterranean N:P ratios and low $\delta^{15}N$-NO_3 values suggest that external nutrient sources such as nitrogen fixation, atmospheric deposition, Saharan dust, and riverine inputs are important controlling factors on the overall nutrient budget (e.g., Krom et al., 2010; Pantoja et al., 2002; Sachs & Repeta, 1999). However, the relative contributions of these sources are debated.

Nitrogen fixation has been proposed to explain the elevated N:P and low $\delta^{15}N$, as fixation produces a source of nitrogen without phosphorus (as well as consuming phosphorus) and a low $\delta^{15}N$ of ~-1‰ reflecting its atmospheric nitrogen source (Carpenter et al., 1997; Minagawa and Wada, 1986). The first Mediterranean nutrient budget studies provided evidence for this (Bethoux and Copin-Montegut, 1986), but studies determining fixation rates across the Mediterranean have reported conflicting results.

Pantoja et al. (2002) found fixation increased eastward, correlating with higher N:P ratios. Using $\delta^{15}N$ isotopes, they inferred significant fixation in the east, contributing up to 90% of the nitrogen supply, compared to 20% in the west. However, atmospheric contributions were not considered. Some depleted $\delta^{15}N$ signals could arise from isotopically depleted DON entering via the Strait of Gibraltar, though Mediterranean DON data are sparse. In contrast, Bonnet et al. (2011), using $^{15}N_2$ tracers, found decreasing fixation rates from west to east, inversely proportional to the N:P ratio, and attributed this to phosphorus limitation in the east, with most productivity driven by atmospheric deposition and, to a lesser degree, river inputs, leaving little scope for diazotrophic contributions. Fixation contributed only 0.4% of external nitrogen inputs in the east versus 25% in the west, supporting 17 - 35% of new production (Bonnet et al.,

https://doi.org/10.5194/egusphere-2026-4372
Preprint. Discussion started: 11 August 2026

2011; Garcia et al., 2006). Similar trends were observed in the aphotic zone, but with reduced effects on total nitrogen inputs (Benavides et al., 2016).

Riverine discharges, while locally significant, are minor in shaping open Mediterranean N:P and isotope ratios (Powley et al., 2017b). Rivers deliver high N:P but enriched $\delta^{15}N$ (6 - 12‰) (Bratek et al., 2020; Johannsen et al., 2008; Mayer et al., 2002) with inputs localised to coastal areas.

Atmospheric deposition is a significant nutrient source in the Mediterranean, receiving some of the highest aeolian deposition rates globally (Guerzoni et al., 1999). During summer stratification, atmospheric inputs dominate surface nutrient supply, influencing productivity and biogeochemistry (Kanakidou et al., 2020; Ridame et al., 2011). Atmospheric depositions have high N:P ratios exceeding Redfield ratios (Markaki et al., 2010), potentially controlling nutrient dynamics over nitrogen fixation (Bonnet et al., 2011; Kanakidou et al., 2020; Krom et al., 2010; Mara et al., 2009; Shelley et al., 2025).

Anthropogenic emissions from European industrial regions and large coastal cities contributes NOx compounds with low $\delta^{15}N$ (-3.1‰ (Mara et al., 2009)) which may influence the overall low Mediterranean $\delta^{15}N$. The $\delta^{15}N$ of atmospheric nitrate increases westward, reflecting greater anthropogenic impact (Mara et al., 2009). Globally, 58 - 65% of atmospheric nitrogen is from an anthropogenic emission source (Fowler et al., 2015; Jickells et al., 2017), with the Mediterranean seeing a greater fraction of up to 85% (Kanakidou et al., 2016, 2020; Nehir and Koçak, 2018).

Saharan dust provides significant phosphorus and trace metals essential for phytoplankton (Guieu et al., 2002; Ridame et al., 2011). It is the primary source of dissolved iron in the Mediterranean (96% of total iron is from atmospheric deposition), preventing iron limitation (Guieu et al., 2002) and provides 30 - 40% of atmospheric phosphorus (Ridame and Guieu, 2002). Dissolved Inorganic Phosphorus (DIP) is a source of bioavailable phosphorus and can relieve surface phosphorus limitation and potentially stimulate nitrogen fixation (Ridame et al., 2011). The extent depends on the composition of diazotrophic communities and their nutrient requirements (Ridame et al., 2022).

Dust deposition peaks in the Eastern Mediterranean in spring, shifting westward in summer (Varga et al., 2014) while winter depositions are significantly reduced. Anthropogenic atmospheric nutrient inputs remain relatively steady year-round (Kanakidou et al., 2020). During the summer stratification period when surface water has the lowest nutrient concentrations due to the low surface mixing rates, external

https://doi.org/10.5194/egusphere-2026-4372
Preprint. Discussion started: 11 August 2026

nutrient inputs are most significant to the nutrient budget. In this period, inputs from both anthropogenic and dust are important.

Differentiating between atmospheric deposition and nitrogen fixation influences on nutrient dynamics is challenging due to their similar high N:P ratios and negative $\delta^{15}N$ signals (atmospheric deposition: -4 to -2‰, fixation: -2.6 to 0‰) (Mara et al., 2009; Wald et al., 2025). Using additional proxies and considering seasonal and spatial variability helps resolve their relative contributions.

Understanding Mediterranean nutrient dynamics requires examining external nutrient sources, surface water changes, and intermediate water formation. Utilising stoichiometry and stable nitrogen isotope ratios of multiple species (nitrate, Total Dissolved Nitrogen (TDN), DON and Particulate Nitrogen (PN)) will show an integrated picture of these processes. This novel approach in a study of Mediterranean biogeochemistry highlights the links between external nutrient inputs to the surface Mediterranean and their export to depth, while further elucidating the controls on nutrient dynamics. This study aims to determine changes in Mediterranean surface water brought in from the Atlantic and to elucidate the roles of atmospheric deposition and nitrogen fixation in determining nutrient ratios and nitrogen isotope composition. We further investigate the processes controlling the nutrient properties of the LIW during its formation and the extent to which these properties are passed to depth.

2 Methods

2.1 Fieldwork and Analyses

Samples were collected from the 2013 GEOTRACES cruise GA04 on board RV Pelagia, of which stations from leg 1 (64PE370 - Lisbon to Istanbul, 14 May - 3 June) and leg 3 (64PE374 - Istanbul to Lisbon, 25 July - 3 August) were used in this study (Rijkenberg, 2013, 2014) (Figure 1a).

Full depth water column samples were collected, filtered from the ship's CTD niskin bottles, and analysed onboard for nutrients (n=834) at each of the 56 stations using a continuous flow auto-analyser following Grasshoff et al. (1983). All other samples for dissolved parameters were collected and filtered from niskin bottles and immediately frozen at -20° C. DOCN concentrations were determined (n=47) using a

https://doi.org/10.5194/egusphere-2026-4372
Preprint. Discussion started: 11 August 2026

Shimadzu TOC-VCPH with nitrogen module TNM-1 and for DOP (n=38), following the high temperature acid persulfate method (adjusted from Davis et al., 2019).

Nitrogen isotopes of nitrate (n=23) were prepared following the Denitrifier Method (Casciotti et al., 2002; McIlvin and Casciotti, 2011; Sigman and Casciotti, 2001) and analysed using a Thermo Scientific Delta V Plus IRMS, coupled to a Thermo Scientific GasBench II and PAL autosampler. Nitrogen isotopes of TDN and DON (n=19) were determined using the same Denitrifier Method, with a prior potassium persulphate oxidation step following Knapp et al. (2005) and Thibodeau et al. (2013), and analysed on an Elementar PrecisION continuous-flow IRMS interfaced with a modified greenhouse gas device (Weigand et al., 2016) and Gilson autosampler. The analytical precision based on the standard deviations of repeat standards was better than ± 0.2‰, and the detection limit was dependent on the concentration limit of the denitrifier method, rather than the instrument limit, with 1µM of nitrate + nitrite being the lowest concentration run to still give reliable results on both repeat samples and standards.

Particulate samples for PN concentration and isotope analysis (n=19) were collected from cruise 64PE374 at the surface using the ship's underway system and at the Deep Chlorophyll Maximum (DCM) using the CTD. Particulates were collected on a 0.7 µm GFF filter through seawater filtration. Analysis was carried out by combusting filters and measuring through an elemental analyser linked to an IRMS, following a method outlined in Tuerena et al. (2021).

The effect of the long-frozen storage time between sample collection (2013) and analysis for nitrogen isotopes and DON concentrations (2023/2024) was assessed by measuring changes in nitrate concentrations. Back calculations using the sample injection volumes and peak areas from the IRMS analysis revealed that concentrations were, on average, 94 ± 14 % (n=57) of the original analysis nitrate values, showing minimal concentration changes due to storage.

Data from CTD casts at each station (salinity, temperature, depth, density, and oxygen concentration) were used to identify and set boundary conditions for individual stations (Figure 1a) and samples in major water masses involved in nutrient dynamics, cycling, and export.

Atmospheric aerosol sample fluxes of soluble Total Inorganic Nitrogen (TIN: nitrate + ammonium), soluble reactive phosphorus and soluble iron measured from samples taken from the same cruise were provided from Shelley et al. (2025). Dry deposition fluxes were calculated as the product of the measured

https://doi.org/10.5194/egusphere-2026-4372
Preprint. Discussion started: 11 August 2026

aerosol concentration and a deposition velocity (1 cm/s used for coarse particles (e.g., mineral dust and seasalt-associated nitrate) and 0.1 cm/s for fine particles (e.g., ammonium)). These fluxes represent an instantaneous snapshot of deposition when wet deposition is minimal during the dry summer months (Shelley et al., 2025). Full details of the collection methods and flux calculations are in Shelley et al. (2025).

2.2 Water mass characterisation

Atlantic water (AW) enters the Mediterranean at the Strait of Gibraltar and develops into MAW through its transport via evaporation increasing salinity and temperature and mixing (Poulos, 2023). For simplicity, this is referred to as MAW for this whole water mass. The inflow of surface MAW spans from the Strait of Gibraltar to the Rhodes Gyre (samples < 150 m depth from leg 1, 64PE370), see Figure 2a. The LIW forms mainly within the Rhodes Gyre. While isotope samples were not collected directly in the formation zone (stations 1-26 to 1-28, CTD only, Figure 2), adjacent stations were used to capture pre- and post-formation signals. Stations 1-21 and 1-24 (64PE370) represent pre-formation MAW, while stations 3-1 and 3-3 (64PE374) represent post-formation MAW and LIW, with intermediate CTD/nutrient-only stations (1-22, 1-23, 1-25; 3-2) providing additional context. Although samples were taken during summer stratification, the isotope signals provide an integrated picture of the average annual nitrogen dynamics of each water mass (Montoya, 2008).

Water mass pathways were assigned based on Millot and Taupier-Letage (2005) and used to assign stations (Figure 2). The division between the Western and Eastern Basins was assigned between stations 1-14 and 1-16 in 64PE370 and between 3-11 and 3-12 in 64PE374.

https://doi.org/10.5194/egusphere-2026-4372
Preprint. Discussion started: 11 August 2026

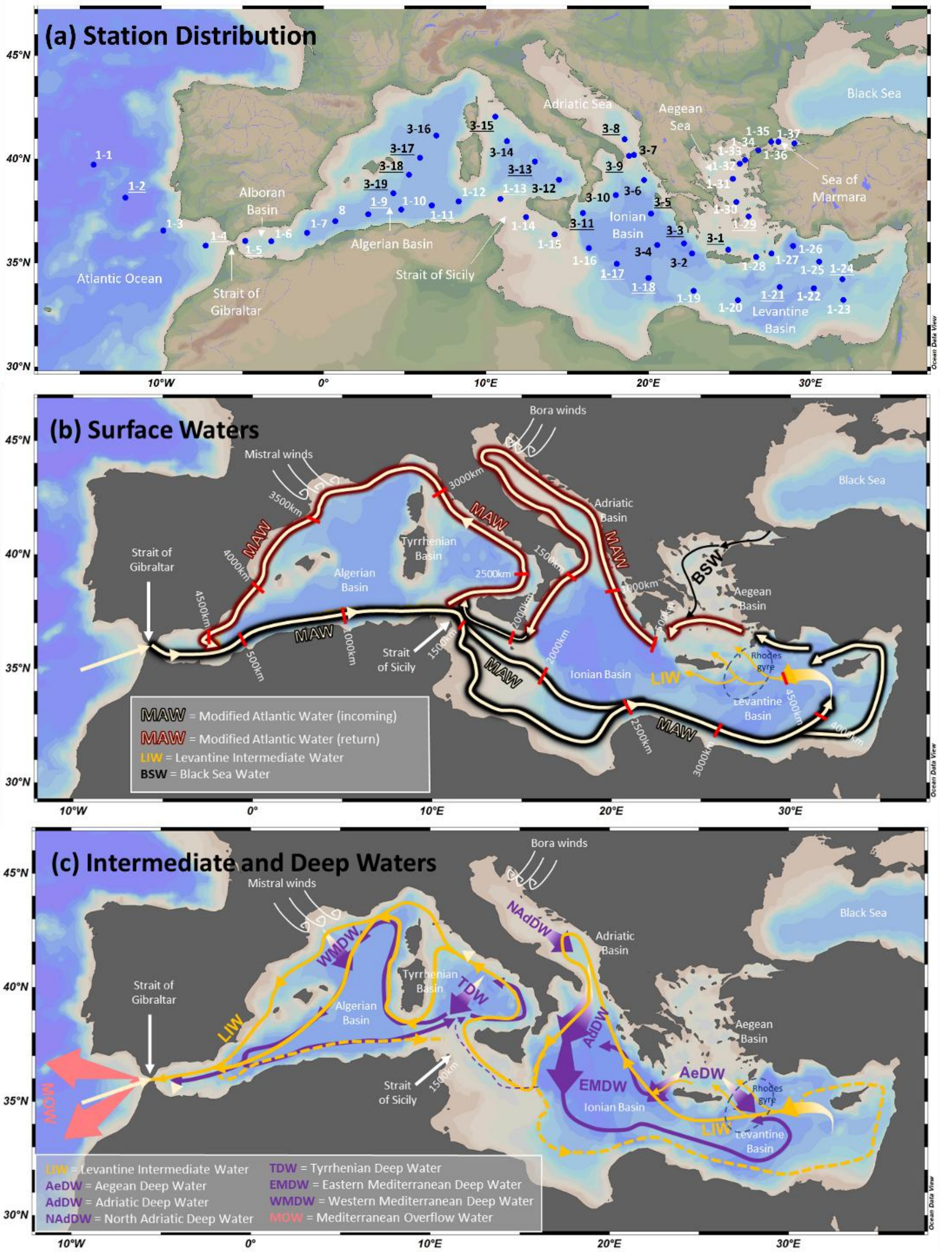

Figure 1 - (a) Map of the Mediterranean Sea showing the station distributions from the 2013 GEOTRACES cruise GA04, leg 1 64PE370 (white font) and leg 3 64PE374 (black font) used in this study. Underlined stations show where samples for isotopic and DOCN analysis were taken while no underlined stations had nutrients analysed only. (b) Surface water circulation map, modified from Millot and Taupier-Letage (2005) showing the incoming Modified Atlantic Water (MAW) (upper 150m) along its path from the Strait of Gibraltar to the LIW formation zone is highlighted in a cream colour with a black outline, while its return flow after LIW formation is highlighted in a cream colour with a red outline. Distances since water mass formation are shown as red lines. Not all of the MAW main path was captured at the cruise sample sites, including within the Adriatic Sea and along the Spanish continental margin. (c) Map showing the intermediate (orange) and deep-water (purple) circulation, modified from Millot and Taupier-Letage (2005) showing the water masses formed from the MAW and their transport pathways.

https://doi.org/10.5194/egusphere-2026-4372
Preprint. Discussion started: 11 August 2026

3 Results

3.1 MAW surface water

3.1.1 Inflow of surface MAW pre LIW formation

Within the surface MAW, flowing eastwards from the Strait of Gibraltar, nitrate and phosphate concentrations are highest (relative to the whole surface Mediterranean) at ~2 - 4 µM and ~0.1 - 0.2 µM, respectively. N* is positive at 0.8 µM (Figure 2d). DON makes up the majority of the TDN pool at 5.3 ± 1 µM (87% of TDN); no DOP was analysed for this initial MAW, but it is likely also to make up the majority of the TDP pool due to the similarity of trends between nitrate and phosphate (Figure 2b).

A fluorescence peak at the MAW origin indicates moderate productivity (Figure 2a). δ^{15}N-TDN was highest here (3.81 ± 0.11‰) (Figure 2e), likely reflecting the surface Atlantic signal of 4.3 - 4.4‰ (data not shown in this study). This organic-rich MAW flows east into the Mediterranean with progressively decreasing inorganic nutrient concentrations and fluorescence. N* peaks at the east end of the western basin along with a minimum in DON before rapidly decreasing into the eastern basin (Figure 2d). Here, most parameters remain stable, with near-zero levels of inorganic nutrients, fluorescence and N*, reflecting the ultraoligotrophic nature of the Eastern Mediterranean. Both nitrogen and phosphorus are almost entirely organic (near 100% DON/P in TDN/P) throughout the basin, with concentrations of 5.32 ± 0.79 µM and 0.32 ± 0.12 µM for DON and DOP, respectively (Figure 2b).

The δ^{15}N-TDN signal progressively decreases, more rapidly at first in the west and then gradually in the east to 2.85 ± 0.02‰ before reaching the LIW formation zone (Figure 2e). The MAW here is rich in organics, poor in inorganics, with a low N* and a low overall δ^{15}N nitrogen signal. These properties will form the LIW during winter convection events.

https://doi.org/10.5194/egusphere-2026-4372
Preprint. Discussion started: 11 August 2026

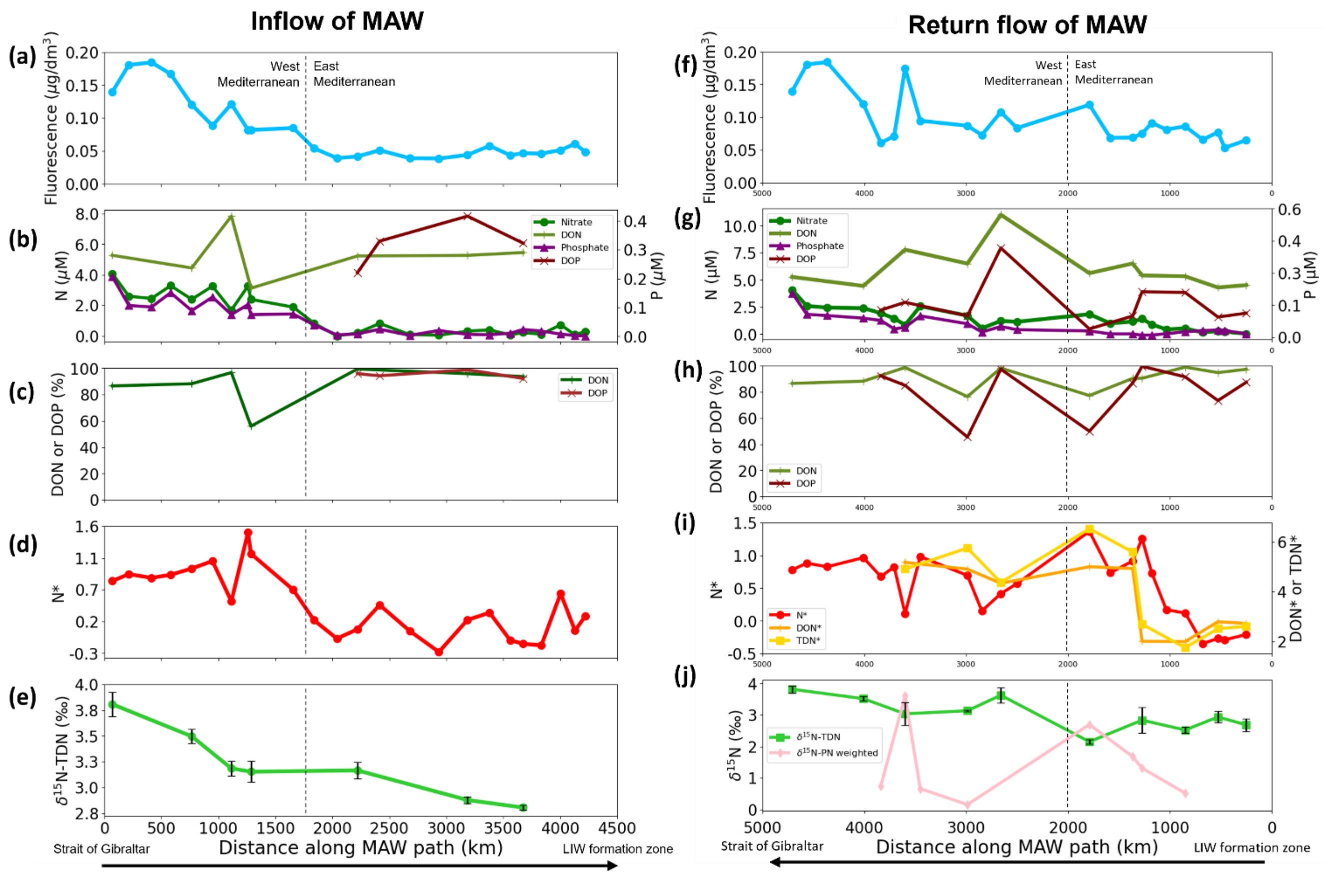

Figure 2 - (a & f) Average fluorescence in the MAW following the flow path in Figure 1b. (b & g) Average concentrations of inorganic nutrients (nitrate and phosphate) and organic nutrients (DON and DOP) in the MAW plotted together to show the relative changes in composition of the TDN and TDP pools. (c&h) Average percentage composition of TDN and TDP made up of DON and DOP, respectively, in the MAW. (d) Average N* in the incoming MAW (i) Average N* DON* and TDN* in the MAW return flow. (e & j) Average δ^{15}N-TDN in the MAW. δ^{15}N-TDN is used to represent the nitrogen isotopic signature because nitrate concentrations are negligible in much of the surface water, so δ^{15}N-NO_3 was not measurable, or if it was, it was often only at the base of the MAW and may not show true surface processes. δ^{15}N-TDN can also be considered as the δ^{15}N-DON, which makes up nearly 100% of the nitrogen pool in the MAW. The concentration-weighted δ^{15}N-PN between the surface and DCM values in the return flow of the MAW is also shown in (j).

https://doi.org/10.5194/egusphere-2026-4372
Preprint. Discussion started: 11 August 2026

3.1.2 Return flow of surface MAW after LIW formation

The MAW return flow in the Northern Mediterranean is the remaining surface water after LIW formation, which flows atop the outgoing LIW. Here, fluorescence increases towards the west, with peaks around 3500 km and 4500 km just before the Strait of Gibraltar (Figure 2f). Inorganic nutrients increase from near-zero in the east to 2.5 µM nitrate and 0.1 µM phosphate in the west. DON and DOP remain relatively constant at 6.23 ± 2.12 µM and 0.16 ± 0.12 µM (Figure 2g).

To assess organic-inorganic interactions, new parameters are defined: DON* = [DON] - 16 × [DOP] and TDN* = [TDN] - 16 × [TDP] (Figure 2i). In the return flow of the surface MAW, N*, DON* and TDN* increase westward (similar to N* in the inflow of surface MAW in Figure 2d). Near the LIW formation region (0 - 1500km), N*, nitrate and phosphate concentrations are close to zero, indicating nutrient deplete surface waters. DON* and TDN* in this region are positive (2 µM) (Figure 2i). DON* and TDN* increase rapidly at around 1300 km, corresponding to the Adriatic influence, and maximum DON* (5 µM), TDN* (6 µM) and N* (1.5 µM) are reached shortly afterwards at the westernmost station of the eastern basin before decreasing slightly in the Western Mediterranean.

No δ^{15}N-NO_3 measurements were possible in the MAW in the whole Mediterranean due to very low nitrate concentrations. As a result, δ^{15}N-TDN can be interpreted as δ^{15}N-DON. The outgoing MAW has an initial δ^{15}N-TDN of 2.7 ± 0.2‰ just after LIW formation - the same (within error) as the δ^{15}N-TDN of incoming MAW to the LIW formation area (Figure 2e), highlighting the stability of the integrated isotope signal over the summer stratification period despite spatial and temporal separation. δ^{15}N-TDN remains stable in the eastern basin but increases in the western basin, reaching 3.04 ± 0.67‰ before mixing with initial MAW input value from the Atlantic (Figure 2e) to reach 3.8 ± 0.11‰ around the Strait of Gibraltar (Figure 2j).

Concentration-weighted δ^{15}N-PN values in the return flow of the MAW at the surface and DCM were averaged to give an overall picture of the δ^{15}N-PN in the surface MAW. This is shown in pink alongside the δ^{15}N-TDN in Figure 2j.

https://doi.org/10.5194/egusphere-2026-4372
Preprint. Discussion started: 11 August 2026

δ^{15}N-PN peaks were observed around 1800 km near the Strait of Sicily and Messina (2.8‰) and at 3600 km in the Western Mediterranean (3.6‰), where the signal matches or exceeds that of the δ^{15}N-DON and coincides with fluorescence maxima. The eastern δ^{15}N-PN maximum aligns with N* and TDN* maxima, while the western δ^{15}N-PN maximum coincides with an N* minima, implying basin-specific processes at play.

PN concentrations were low (0.2 - 0.5 µM) for both surface and DCM (Fig. A1), with a single peak of 1.2 µM coinciding with δ^{15}N-PN and fluorescence maxima. Therefore, most of the surface TN pool is represented by DON, which is relatively homogeneous across the whole MAW.

Given the similar nutrient and isotopic longitudinal trends in incoming and return flow MAW (Figure 2), it is reasonable to assume that similar processes affect the entire surface Mediterranean. Similar trends would therefore be present in the incoming MAW for DON* and TDN*; so, the interpretations in Sect. 4.1 apply to the whole surface Mediterranean.

3.2 Atmospheric inputs

A combination of observed daily aerosol dry deposition fluxes and their corresponding modelled annually averaged deposition fluxes was used to determine the contributions of atmospheric soluble nitrogen, phosphorus and iron deposition across the Mediterranean (Figure 3). The solubility of atmospheric phosphorus and iron is low (particularly when associated with Saharan dust), so total deposition of these nutrients will be greater than considered here (Shelley et al., 2025). Table 1 shows median and range values of measured and modelled N, P and N:P depositions for the Western and Eastern Mediterranean basins along with the differences in deposition between the basins.

The highest TIN dry deposition fluxes (Figure 3a) generally occur in the Western Mediterranean, with the SE portion seeing the peak of 300 µmol m^{-2} d^{-1}, and a western basin median of 186 µmol m^{-2} d^{-1}, significantly higher than the median of 116 µmol m^{-2} d^{-1} in the east (Mann-Whitney U, $p = 0.043$) (Table 1). The modelled annually averaged Dissolved Inorganic Nitrogen (DIN) deposition (including gas-phase, dry aerosol and wet deposition) modified from Kanakidou et al. (2020) (Figure 3b) are also significantly greater in the Western Mediterranean (median of 29 vs 16 mmol N m^{-2} yr^{-1}, $p = 0.003$) (Table 1). However, peak depositions occur in coastal regions in closer proximity to cities and industry, with the Northern

https://doi.org/10.5194/egusphere-2026-4372
Preprint. Discussion started: 11 August 2026

Adriatic having the maximum deposition rate (~100 mmol N m^{-2} yr^{-1}). The greatest deposition away from coastal regions occurs in the SE western Mediterranean (~40 mmol N m^{-2} yr^{-1}), a similar region to the greatest TIN depositions (Figure 3a). The open Eastern Mediterranean, away from coastal regions, shows lower annual deposition rates (~15 to 20 mmol N m^{-2} yr^{-1}).

The atmospheric soluble PO_4 flux (Figure 3c) shows a more sporadic distribution with areas of both the Western and Eastern Mediterranean showing high and low fluxes. The maximum deposition (189 nmol m^{-2} d^{1}) occurs at station 21 corresponding to a localised Saharan dust deposition event during the cruise (Rijkenberg, 2013; Shelley et al., 2025) suggesting a Saharan dust source. The east has a greater median deposition than the west (71 vs 48 nmol m^{-2} d^{-1}), but this difference is not statistically significant ($p = 0.141$) (Table 1) due to the large overlapping ranges of depositions rates.

Modelled annually averaged Dissolved Inorganic Phosphorus (DIP) deposition (Figure 3d) also shows no significant difference between the basins ($p = 0.943$) (Table 1) but has the greatest depositions nearest the coast of Africa and in the Southern Adriatic.

The atmospheric soluble iron flux (Figure 3e) and modelled annually averaged Dissolved Iron (DFe) (Figure 3f) both show a similar picture with mostly uniform depositions across the east and west. The far eastern portion of the east basin shows the lowest annually averaged deposition while the western basin shows some sporadic maxima in measured deposition fluxes.

The combined measured N and P fluxes as the N:P ratio (Figure 3g) was significantly greater in the west than the east (TIN: PO_4 3707 mol mol^{-1} vs 2162 mol mol^{-1}, $p = 0.015$) (Table 1). The modelled annually averaged N:P ratio was also significantly greater in the west (DIN:DIP 904 mol mol^{-1} vs 437 mol mol^{-1}, $p < 0.001$) (Table 1). The differences in magnitudes between the measured and modelled N:P ratios is presumably at least partly due to the differences in N and P species included in each deposition estimate. The consistency of the patterns in measured and modelled deposition data supports the robustness of the increased stoichiometrically-enriched nitrogen deposition in the Western Mediterranean in both short term and annual deposition. The high degree of significance (low p-values) suggests that trends are likely true even with the rough approximation approach when comparing the modelled data (Table 1 caption).

https://doi.org/10.5194/egusphere-2026-4372
Preprint. Discussion started: 11 August 2026

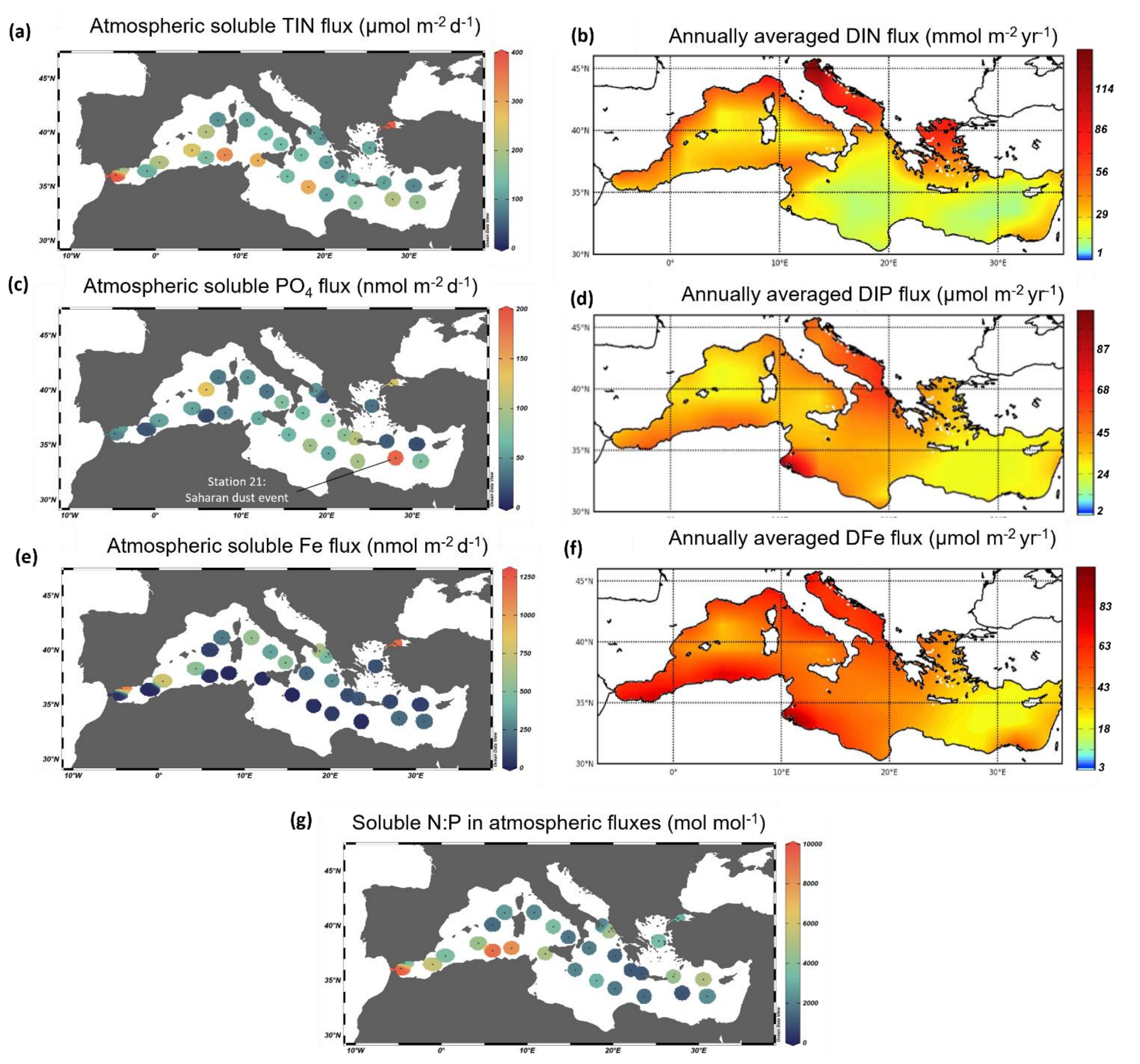

Figure 3 - Measured atmospheric deposition fluxes measured during the GA04 cruise and modelled annually averaged fluxes. (a) Soluble Total Inorganic Nitrogen (TIN) flux from anthropogenic atmospheric deposition to the Mediterranean. Sampling points (black dots) are not interpolated because the depositions only provide a snapshot and would change too much to be spatially interpolated. (b) Modelled annually averaged atmospheric DIN flux. (c) Atmospheric soluble phosphate fluxes from aerosol deposition across the Mediterranean. (d) Modelled annually averaged atmospheric DIP flux (e) Atmospheric soluble iron fluxes from aerosol deposition across the Mediterranean. (f) Modelled annually averaged atmospheric DFe flux. (g) N:P ratios of the atmospheric fluxes across the Mediterranean. Data in (a), (c), (e) and (g) are from Shelley et al., 2025. Plots in (b), (d) and (f) are modified from Kanakidou et al. (2020).

https://doi.org/10.5194/egusphere-2026-4372
Preprint. Discussion started: 11 August 2026

		TIN Measured (µmol m^{-2} d^{-1})	DIN Modelled (mmol m^{-2} yr^{-1})	PO_4 Measured (nmol m^{-2} d^{-1})	DIP Modelled (mmol m^{-2} yr^{-1})	N:P Measured (mol mol^{-1})	N:P Modelled (mol mol^{-1})
West	Median	186	29	48	0.032	3707	904
	Range	95 - 399	23 - 40	16 - 132	0.026 – 0.042	1600 - 9672	732 - 1127
East	Median	116	16	71	0.034	2162	437
	Range	91 - 297	9 - 21	18 - 189	0.026 – 0.048	1088 - 5103	313 - 653
West/East difference		70 ($p = 0.043$)	13 ($p = 0.003$)	23 ($p = 0.141$)	-0.002 ($p = 0.943$)	1545 ($p = 0.015$)	467 ($p < 0.001$)

Table 1 - Table of median and ranges of measured TIN, PO_4, N:P across the Mediterranean from the GA04 cruise and equivalent modelled DIN, DIP and N:P from Kanakidou et al. (2020). Median values were used rather than means to reduce the influence of outlying points, which are common in this data. Modelled values from Kanakidou et al. (2020) were obtained from choosing 6-7 evenly distributed points in each of the west and east basins from figures showing annual modelled DIN and DIP and reading values from the figure key. The difference between the west and the east basin is shown with associated p-values calculated via the Man-Whitney U-test to demonstrate statistical significance (green) or insignificance (red).

3.3 LIW formation area

The stations around the LIW formation site within the Rhodes Gyre were grouped based on the MAW to LIW flow paths (Figure 4a) to track nutrient changes in MAW as it forms LIW (see Sect. 2.2)

In both incoming and outgoing MAW, nitrate and phosphate concentrations were near or below the limit of detection (Figure 4b & c), making N* effectively zero where concentrations are near the detection limits but undeterminable when below detection limits. During LIW formation, N* increases (from 0 µM) with concordant nitrate and phosphate concentrations (nitrate: 0.25 to 2.34 µM, phosphate: 0.01 to 0.08 µM).

Due to the low concentrations of nitrate and phosphate, the inorganic contributions to TDN and TDP are almost negligible and observing the organic portion in the MAW would be more representative of nutrient dynamics here and indeed sees the most significant differences between incoming (MAW) and outgoing water masses (MAW return flow and LIW). DON* increases from -0.54 ± 1.06 µM in pre-formation MAW to 2.75 ± 1.06 µM post-formation, comparable to the newly formed LIW value of 3.34 ± 1.18 µM (Figure 4d). This increase is mainly due to a reduction in DOP (0.37 to 0.09 µM), while DON remains stable from the incoming MAW to the outgoing MAW and LIW (Figure 4b & c). This suggests that DOP is preferentially removed over DON, raising DON* in surface MAW and newly formed LIW.

The δ^{15}N-DON shows no change through MAW circulation or LIW formation (2.85 ± 0.41‰) (Figure 4e). This follows the constant trend of the DON concentrations but is lower than previous estimates of

https://doi.org/10.5194/egusphere-2026-4372
Preprint. Discussion started: 11 August 2026

δ^{15}N-DON (Wald et al., 2025) but similar to some δ^{15}N of total reduced nitrogen, mostly made up of DON (Emeis et al., 2010). Nitrate concentrations were below detection in the upper 80 m around the Rhodes Gyre (Fig. A2) so again, all TDN is represented by DON for concentrations and isotopes. Between 80 - 150 m, nitrate concentrations increase slightly to ≤1 µM with concomitant high δ^{15}N (Wald et al., 2025), but this comprises only a small proportion compared to DON in MAW with concentrations of 4.5 - 5.5 µM (Figure 4b).

δ^{15}N-PN in the outgoing MAW beyond the Rhodes Gyre is low at 0.73 ± 0.3‰, much lower than δ^{15}N-DON (2.81 ± 0.13‰), aligning with previous observations of low or negative δ^{15}N-PN in this area within the MAW (e.g., -0.57‰ - Pavlidou et al., 2020)). Although δ^{15}N-PN data were unavailable for the incoming surface MAW or LIW, the unchanging δ^{15}N-DON across the formation zone (Figure 4e) suggests δ^{15}N-PN is also unchanging, as DON and PN have similar influencing processes, and therefore it is assumed that around the LIW formation area, δ^{15}N-PN in outgoing MAW = δ^{15}N-PN in incoming MAW. PN concentrations (0.44 µM) exceed nitrate but are lower than DON, indicating that most nitrogen is in the dissolved organic phase rather than the particulate.

Once the LIW forms at depths between 150 and 700 m, nitrate concentrations increase to 2.33 ± 1.03 µM with low δ^{15}N-NO_3 at 1.66 ± 0.17‰, falling between the MAW values for δ^{15}N-DON and δ^{15}N-PN. These initial low δ^{15}N-NO_3 LIW values are similar to past observations (e.g., 1.11‰ - Pavlidou et al., 2020).

https://doi.org/10.5194/egusphere-2026-4372
Preprint. Discussion started: 11 August 2026

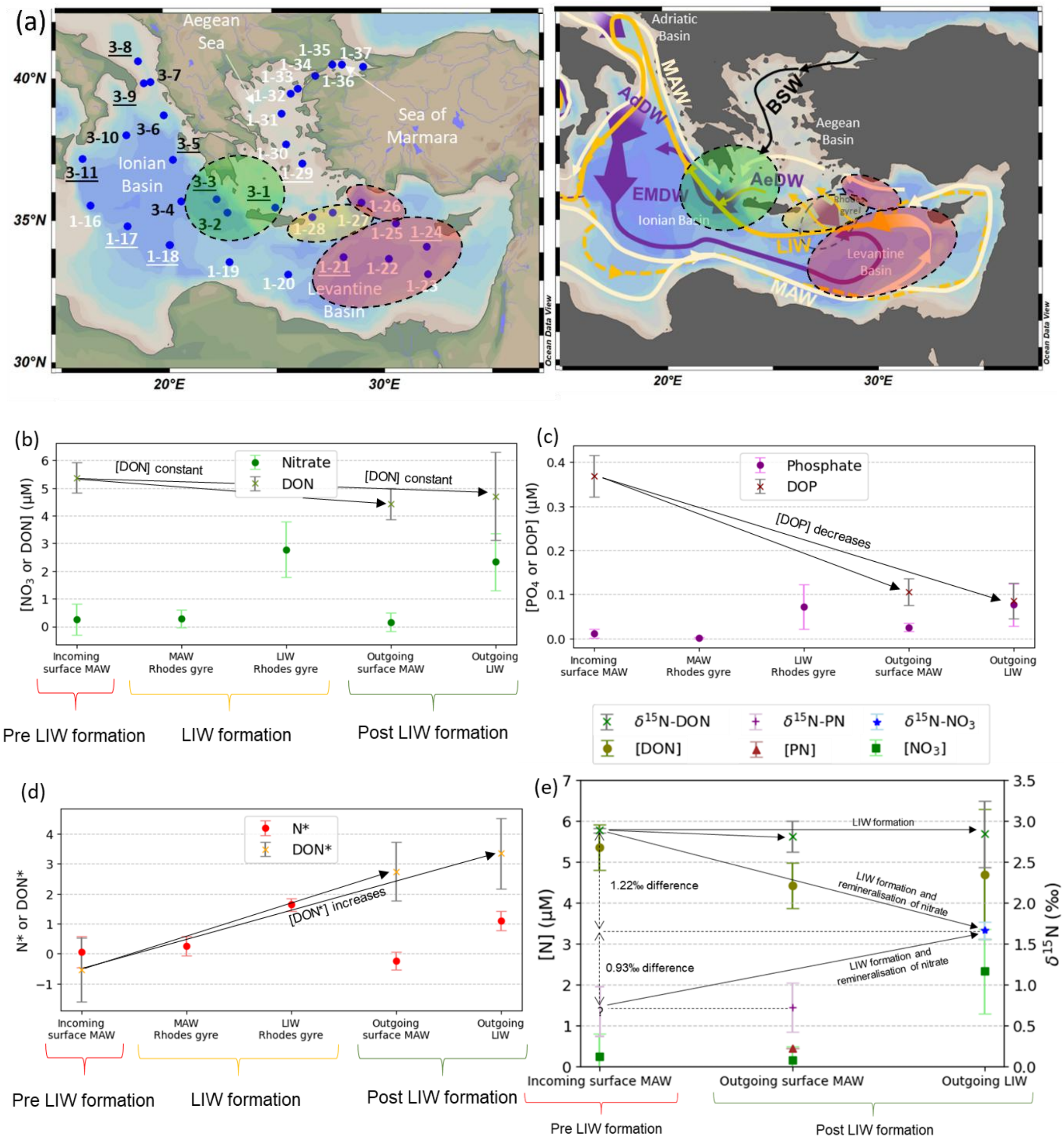

Figure 4 - (a) Map of the Eastern Mediterranean showing the stations selected for the LIW formation zone comparison following the water mass circulation in that area. Red = Pre-LIW formation, orange = LIW formation site (Rhodes's gyre) and Green = Post-LIW formation. (b) Average nitrate and DON concentrations. (c) Average phosphate and DOP concentrations. (d) Average N* and DON* values. (e) Averaged stable nitrogen isotope ratios ($\delta^{15}N$) and concentrations of DON, PN, and nitrate within each water mass. Error bars represent one standard deviation from the calculated means. The same defining water mass characteristics were used as described in Sect. 2.2.

https://doi.org/10.5194/egusphere-2026-4372
Preprint. Discussion started: 11 August 2026

4 Discussion

4.1 Influence of external inputs on MAW properties

The incoming surface MAW is initially changed due to mixing with underlying Mediterranean waters soon after the Strait of Gibraltar, leading to a peak in productivity via nutrient injection in the Western Alboran Sea (Gómez et al., 2000). After this mixing zone, external sources of nutrients become increasingly important in the MAW, especially during the summer stratified period (Mara et al., 2009; Ridame et al., 2011).

N:P ratios in atmospheric deposition over the Mediterranean are significantly higher than in dissolved surface water ratios of the Mediterranean or the global ocean. This elevated ratio has been proposed to contribute to the phosphate-limited conditions of the Eastern Mediterranean (Krom et al., 2010; Shelley et al., 2025).

To investigate the potential influence of anthropogenic and Saharan dust-derived deposition on nutrient dynamics in the incoming surface water, the average MAW N* was plotted against the atmospheric deposition N:P ratio and the atmospheric TIN deposition flux (Figure 5). A significant positive correlation ($p < 0.05$) between N* in the incoming MAW and atmospheric TIN deposition and the N:P, suggests the ratio of atmospheric nitrogen and phosphorus deposition may be influencing the N* of the MAW during its eastwards transport. Greater nitrogen deposition and higher N:P in the west (Table 1) could increase N*, and a reduced nitrogen deposition and lower N:P in the east could lower N* in MAW to within error of zero. The increased anthropogenic sources of nitrogen in the west may be leading to deposition that is greater than the nutrient requirements of the surface water and elevating N* as a result. Increased mixing in the western basin may also aid the higher N* along with this deposition. The forcing of atmospheric nitrogen deposition likely becomes weaker moving east where Saharan dust derived deposition has an increased contribution of phosphorus (relative to nitrogen, reduced N:P), so the excess nitrogen deposition is reduced to a level where nutrient requirements are not exceeded and MAW N* is reduced to zero (along with lower MAW nutrient concentrations) as a result.

Approximately equal annually averaged iron depositions across the west and east (Figure 3f) provides sufficient iron for biological processes and would not be a limiting nutrient in either basin.

https://doi.org/10.5194/egusphere-2026-4372
Preprint. Discussion started: 11 August 2026

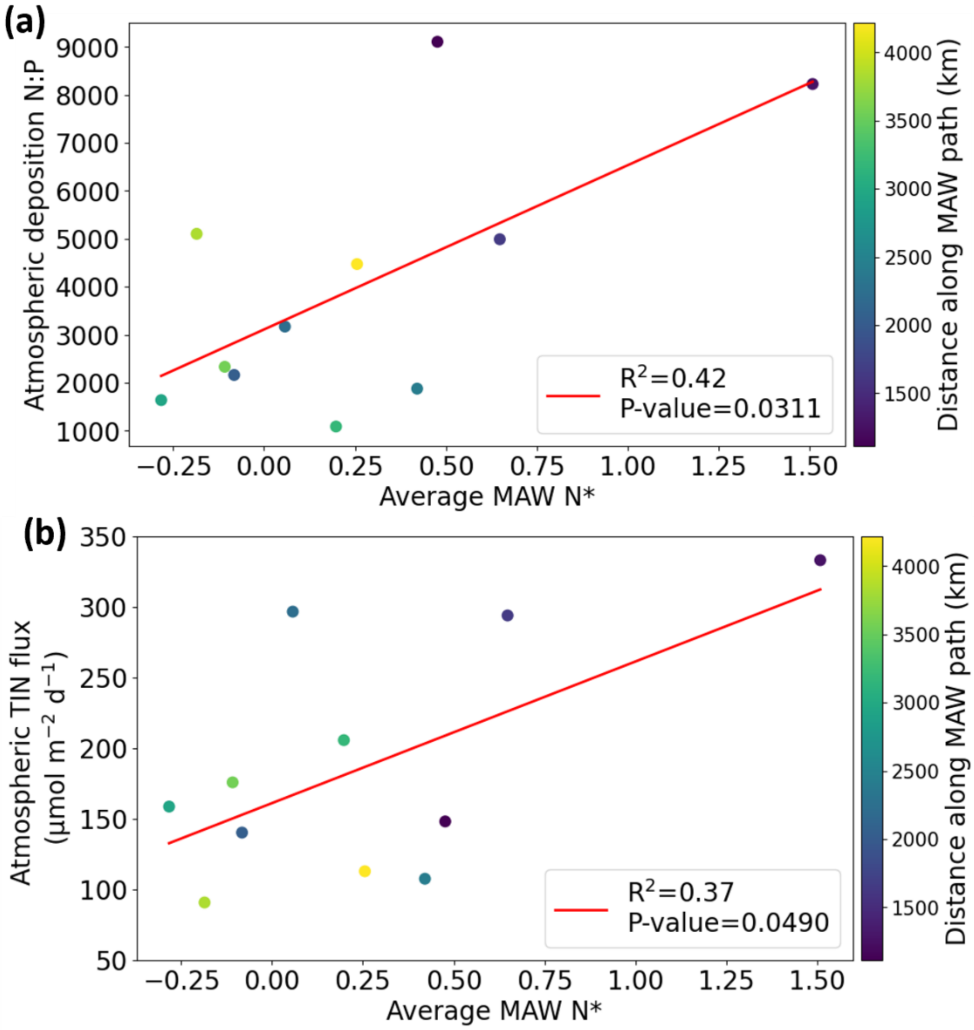

Figure 5 - The average N* for the incoming MAW vs (a) atmospheric deposition N:P ratio, (b) the atmospheric TIN flux (a proxy for anthropogenic deposition). Note that two stations nearest to the Strait of Gibraltar have been excluded to reduce the influence of mixing with the underlying LIW. A significant correlation of N* and TDN* and a justification on the use of N* over TDN* to represent surface processes is given in Fig. A3. An extended set of these figures is available in Fig. A4, showcasing that the same correlations are mostly still statistically significant when considering both the incoming and outgoing N* trends together. Only the incoming MAW N* is shown here to see the changes occurring as surface water is transported towards the LIW formation area.

Atmospheric inputs also affect nitrogen isotope composition in the MAW. The decreasing δ^{15}N-TDN signature (Figure 2e) suggests an external low δ^{15}N input or a change to atmospheric isotopic composition across the Mediterranean. Mara et al. (2009) (and references therein) argue that a longitudinal change in the composition of NO_x in dry deposition during summer stratification results in the Western Mediterranean having a more positive δ^{15}N signature (> 0‰) (Freyer, 1991; Putaud et al., 2004) while in the Eastern Mediterranean, the deposition of DIN shows more negative $\delta^{15}N$ ($\delta^{15}N$-NO_3 of -3.1‰; Mara et al., 2009) significantly lower than the positive values measured in the Western Mediterranean. This gradient from more positive $\delta^{15}N$ deposition in the west to negative $\delta^{15}N$ in the east corresponds to the decreasing isotopic gradient of $\delta^{15}N$-TDN in the MAW observed in this study (Figure 2e) and to changes in anthropogenic DIN deposition rates discussed above.

In the oligotrophic Mediterranean, rapid nitrogen recycling likely links DIN deposition and DON dynamics, transferring isotope signatures with minimal fractionation due to the absence of residual DIN (Altabet and Francois, 1994; Pujo-Pay et al., 2011; Wald et al., 2025).

The measured $\delta^{15}N$-TDN reflects a mix of Atlantic-derived refractory DON and newly formed DON from atmospheric DIN, with the decreasing $\delta^{15}N$-TDN trend in the MAW likely driven by changing $\delta^{15}N$ of deposited DIN during eastward transport. The sharpest $\delta^{15}N$-TDN decrease is observed in the western basin, consistent with high DIN deposition, while the eastern basin shows a weaker gradient.

The potential influence of nitrogen fixation should also be considered in controlling nutrient dynamics and isotopic ratios of nitrogen compounds in the MAW. Nitrogen fixation has been measured across both Mediterranean basins (Benavides et al., 2016; Bethoux and Copin-Montegut, 1986; Bonnet et al., 2011; Ibello et al., 2010; Rahav et al., 2013a) and would decrease the $\delta^{15}N$-TDN due to the low $\delta^{15}N$ atmospheric source of nitrogen (Carpenter et al., 1997; Minagawa and Wada, 1986; Pantoja et al., 2002; Wald et al., 2025). Higher fixation rates have been measured in the west, with decreasing rates further east (Rahav et al., 2013a; Ridame et al., 2011, 2022). This may be due to the presence of inorganic nutrients brought in from the Atlantic or upwelled near the Strait of Gibraltar, alleviating phosphorus limitation (Ridame et al., 2022). However, some studies have measured or hypothesised higher nitrogen fixation rates in the east (Pantoja et al., 2002; Rees et al., 2006; Sachs and Repeta, 1999), leaving this as an ongoing debate. In general, the rates of ambient nitrogen fixation (without external stimulation from dust deposition) in the open ocean of the Mediterranean are lower than the atmospheric deposition flux of nitrogen (≤ 0.5 nmol N L^{-1} d^{-1}) (Benavides et al., 2016; Bonnet et al., 2011; Ibello et al., 2010; Rahav et al., 2013a; Ridame et al., 2011).

Atmospheric deposition of Saharan dust also stimulates nitrogen fixation in phosphorus-limited surface waters by supplying iron and phosphorus and is an important process in the Mediterranean. Ridame et al.

https://doi.org/10.5194/egusphere-2026-4372
Preprint. Discussion started: 11 August 2026

(2022) demonstrated this influence was strongest where non-cyanobacterial diazotrophs (NCDs) dominate, and nutrient limitation is most extreme, conditions found in the ultraoligotrophic eastern basin. The influence was reduced when the photo-heterotrophic group A (UCYN) was the dominant diazotroph species and where higher ambient nutrient concentrations were present, conditions found in the Western Mediterranean. Nitrogen fixation rates can be strongly elevated locally in dust events. Kanakidou et al. (2020) modelled the nitrogen fixation stimulated by dust DIP additions as 70 - 215 Gg N y^{-1} across the Mediterranean, 6 - 18 times lower than atmospheric nitrogen deposition. However, they argue that when considering dissolved iron and DIP inputs together, the resulting potential fixation rates can be of the same order as atmospheric nitrogen deposition across the Mediterranean, though with considerable uncertainty. Considering the Western and Eastern Mediterranean separately, the West would exhibit a more pronounced anthropogenic atmospheric N-dominated signal over stimulated nitrogen fixation. However, when considering only the east, with reduced atmospheric anthropogenic N sources and a lower N:P (Table 1), dust-stimulated nitrogen fixation may have a greater contribution and may exceed atmospheric nitrogen deposition inputs. However, the large uncertainties associated with this suggest that the most likely control on overall nitrogen inputs across the Mediterranean is changing anthropogenic inputs and distributions, with stimulated nitrogen fixation influencing only the eastern-most portion of the Mediterranean (around the LIW formation areas in the Rhodes gyre), most affected by dust inputs and with the lowest DIN depositions.

By the time the MAW reaches the LIW formation area, it carries a signal shaped by this transition: low or negative N*, dominance of organic nitrogen and phosphorus species, and a markedly lower δ^{15}N-TDN (represented mainly by DON) compared to the original Atlantic source. External sources of nitrogen into the MAW would likely be reflected in δ^{15}N-PN (Figure 2j), as it shows a snapshot of the highly labile PN pool. The generally low δ^{15}N-PN across the Mediterranean would reflect atmospheric and fixation-derived nitrogen, while the δ^{15}N-PN peaks, which align with productivity and matching δ^{15}N-TDN, may result from atmospheric nitrogen and phosphorus deposition stimulating productivity and rapid recycling. Though δ^{15}N-PN was only measured in outgoing MAW, similar overall nitrogen dynamics across the surface water (Sect. 3) suggest these values apply more broadly, including the incoming MAW influencing the LIW formation area.

https://doi.org/10.5194/egusphere-2026-4372
Preprint. Discussion started: 11 August 2026

The final characteristics of the incoming MAW in the far Eastern Mediterranean influence the biogeochemistry of the LIW that forms from this water mass in winter convective events within the Rhodes Gyre. Further in-depth evaluation of the processes occurring in this region is important to understand how the LIW develops its overall nutrient properties.

4.2 The role of nitrogen fixation around the LIW formation area

The difference in the $\delta^{15}N$ of DON in the incoming MAW and the nitrate of the exported LIW suggests that the low $\delta^{15}N$ of nitrate cannot be explained by just recycling from DON alone. If this were the case, nitrate would be expected to have the same $\delta^{15}N$ signal as the DON from which it originated prior to remineralisation. The MAW $\delta^{15}N$-PN signal is low and would help lower the $\delta^{15}N$ of the remineralised nitrate in the LIW. However, the concentration of PN is much lower than DON (Figure 4e), so its contribution to the final $\delta^{15}N$-NO_3 value would be limited.

DON remineralisation to ammonium has a small or absent fractionation signal, and the significant fractionation factor that can occur during partial nitrification of ammonium to nitrate would not be present due to ammonium being consumed in Mediterranean waters (Emeis et al., 2010), leaving no residual pool. Therefore, if fractionation or combined DON and PN cycling cannot fully explain the 1.22‰ difference in $\delta^{15}N$ between DON and nitrate, there must be an additional source that is supplying a low $\delta^{15}N$ nitrate signal observed in the LIW nitrate.

Around the LIW formation site in the Rhodes Gyre, the changes observed in the N* and DON* from the incoming MAW to the outgoing LIW and MAW can help to explain the origin of this low $\delta^{15}N$ signal. Observations in Sect. 3.3 demonstrate the removal of DOP over DON in the Rhodes Gyre, which increases the DON* of outgoing LIW and MAW. This suggests that DOP conversion to DIP could stimulate productivity and nitrogen fixation in this phosphorus-limited (or nitrogen and phosphorus co-limited) region of the Mediterranean. The consumption of DOP may be due to the presence of alkaline phosphatase enzymes, the activity of which (Alkaline Phosphatase Activity - APA) can break down DOP and assist microbes in obtaining inorganic phosphorus from DOP and help diazotrophs alleviate phosphorus-limitation and support nitrogen fixation (Letscher and Moore, 2015). Recent studies (Van Wambeke et al., 2024a, b) measured the presence of two alkaline phosphatase enzymes, phosphomonoesterase (PME)

https://doi.org/10.5194/egusphere-2026-4372
Preprint. Discussion started: 11 August 2026

and phosphodiesterase (PDE), involved in ectoenzymatic hydrolysis of DOP by microorganisms within the Eastern Mediterranean. This study was based on an increase in PME activity observed when DIP concentrations decreased below a threshold, as reported in other oligotrophic and phosphorus-limited areas such as the Sargasso Sea and Mediterranean (Lomas et al., 2010; Van Wambeke et al., 2002).

In the Eastern Mediterranean, the nitracline is shallower than the phosphacline (80 m vs 200 m) (Fig. A2), resulting in winter mixing events that form the LIW reaching the nitracline but not the deeper phosphacline, providing a seasonal supply of nitrogen but not phosphorus from depth (Ben Ezra et al., 2021). Alternative phosphorus sources must be available to maintain year-round productivity.

Van Wambeke et al., (2024a) reported PDE activity reached its maximum in winter at stations near the Rhodes Gyre, where DIP concentrations were lowest. Lower rates and ranges of PME and PDE activity were observed in summer stratified conditions, possibly due to nitrogen and phosphorus co-limitation, as nitrogen is needed for cells to produce PME and PDE enzymes (Van Wambeke et al., 2024a). However, highly significant negative correlations existed between the activity rates of PME and PDE and the DIP concentration in each season ($p<0.001$, (Van Wambeke et al., 2024b)), suggesting that DOP hydrolysis occurs in the Rhodes Gyre in both stratified and winter mixed conditions, albeit to a greater extent in winter, whenever DIP concentrations reach their lowest.

Surface DIP concentrations in this study (phosphate) were at their lowest around the Rhodes Gyre (Figure 4c) and Fig. A2). The decrease in DOP concentration and increase in DON* across the gyre may well indicate that DOP hydrolysis through APA was occurring around the time of sampling. They likely influenced the LIW formation in the winter prior to cruise measurements. This production of DIP (which would not be measured due to immediate consumption) may stimulate nitrogen fixation and explain the low $\delta^{15}N$ nitrate signal in the LIW, as nitrogen fixation produces this characteristic nitrate signal. Indeed, nitrogen fixation rates have been measured up to 10 times higher in the Rhodes Gyre than in surrounding water, with rates up to 20 µmol N m^{-2} d^{-1} (Rahav et al., 2013b) recorded in summer stratified conditions. This suggests that modest amounts of DOP hydrolysis in summer/autumn stratified conditions may supply enough DIP to stimulate nitrogen fixation in the Rhodes Gyre/ LIW formation region.

https://doi.org/10.5194/egusphere-2026-4372
Preprint. Discussion started: 11 August 2026

The potential APA rate that may explain the observed loss of DOP was calculated using the published global dataset of APA rates for the Mediterranean (Su et al., 2023) and comparing it to the corresponding DIP concentrations (Figure 6).

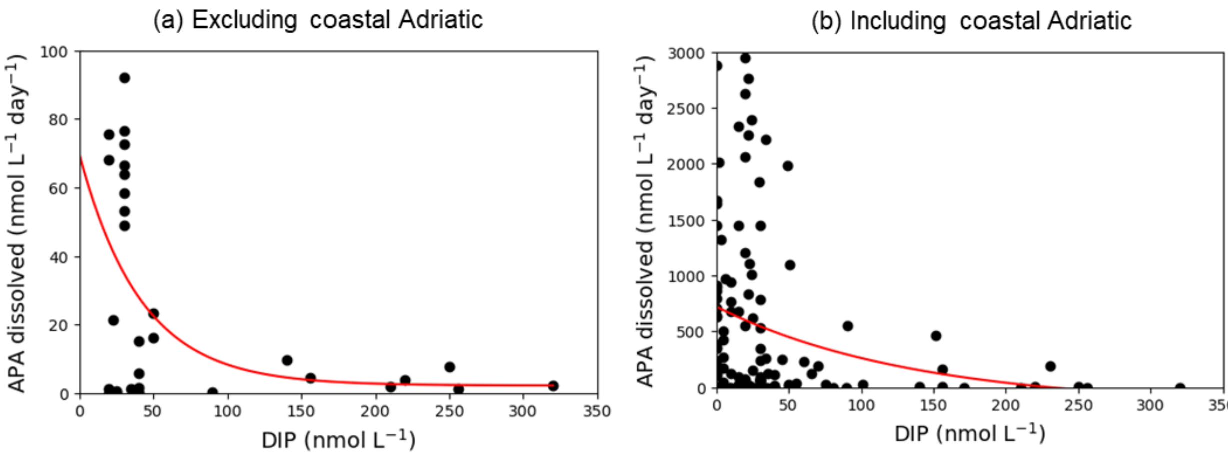

Figure 6 - Relationships between Mediterranean APA rates and the DIP concentrations taken from the dataset of global ocean alkaline phosphatase activity (Su et al., 2023). Most measurements were taken in the coastal Adriatic, which may have a different regime from the rest of the Eastern Mediterranean but has lower DIP concentrations, similar to concentrations in the Rhodes Gyre. Two plots are shown (excluding (a) and including (b) coastal Adriatic samples) to represent different APA and DIP relationships in the Mediterranean.

This dataset does not contain rate measurements from the Rhodes Gyre and exhibits seasonal variability. It gives an approximation of the expected relationships, and the negative exponential relationship obtained is similar to other parts of the global ocean (Mahaffey et al., 2014). Utilising the equation from this relationship, the potential APA rate from the very low DIP concentrations found in the surface of the Rhodes Gyre can be predicted. The mean DIP concentration in the MAW is 1.72 nM, which corresponds to an APA rate (consuming DOP, producing DIP) of 67 nM P day^{-1} (0.067 µM P day^{-1}) (Adriatic excluded) or 712 nM P day^{-1} (0.7 µM P day^{-1}) (Adriatic included).

The measured 0.28 µM (280 nM) change in DOP concentrations across the Rhodes Gyre (Figure 4c) could be explained by these estimated APA rates of DOP conversion to DIP. Using the most conservative estimate of APA rates in the Mediterranean (66.96 nM P day^{-1}) for concentrations found in the Rhodes Gyre, the DOP change observed could occur in just over four days. Using the higher measured rate (712.18 nM P day^{-1}), the DOP change could occur within one day. Whichever estimate of Mediterranean APA rates is used, the APA conversion could explain the observed change in DOP concentrations several

https://doi.org/10.5194/egusphere-2026-4372
Preprint. Discussion started: 11 August 2026

times over. Although other processes likely contribute to changes in DOP and DIP dynamics in the Rhodes Gyre during LIW formation, evidence from APA studies across the Mediterranean supports a substantial contribution of this process to influencing phosphorus dynamics in this area.

Modelling the global ocean suggests that up to 26% more nitrogen fixation can be induced from DOP utilisation via APA, particularly in regions with elevated surface iron concentrations, such as the Atlantic (Letscher and Moore, 2015). The Rhodes Gyre shares key features with Atlantic subtropical gyres, including persistent phosphorus limitation or nitrogen and phosphorus co-limitation, and substantial iron input, suggesting it may also support significant nitrogen fixation fuelled by DOM cycling.

However, other possible sources of DIP to the surface ocean, apart from DOP hydrolysis, could stimulate nitrogen fixation or otherwise supply nitrogen with a low $\delta^{15}N$ signal. Atmospheric deposition must be considered, as many studies argue it could have a more substantial influence on nitrogen dynamics than nitrogen fixation in the Eastern Mediterranean (e.g., Bonnet et al., 2011; Kanakidou et al., 2020; Krom et al., 2010; Mara et al., 2009; Shelley et al., 2025)

As discussed in Sect. 4.1, the Eastern Mediterranean receives a significantly lower N:P through atmospheric deposition compared to the western basin (though always much greater than N:P in surface water) due to a reduction in anthropogenic nitrogen supply. Overall, however, both nitrogen and phosphorus fluxes are significant across the Mediterranean, with atmospheric deposition providing a consistent external nutrient source. Around the Rhodes Gyre, the reduced nitrogen fluxes likely limit the influence of anthropogenic atmospheric nitrogen relative to the Western Mediterranean.

The patchy nature of Saharan dust deposition complicates predictions of where and when external phosphorus inputs may stimulate nitrogen fixation. As shown in Figure 3c, a dust event supplied soluble phosphate at 190 nmol m^{-2} d^{-1}, well above the median of 71 nmol m^{-2} d^{-1}. Such dust events would alleviate phosphorus limitation in the surface water, promoting nitrogen fixation and/or phytoplankton blooms (Ridame et al., 2011, 2022).

While dust events are important, a larger share of Dissolved Phosphorus (DP) in the Eastern Mediterranean is derived from European aerosols as DOP, delivering 3.5 times more DP than desert dust (Longo et al., 2014). Estimates suggest that 44 - 92% of this deposited phosphorus is in the form of DOP

https://doi.org/10.5194/egusphere-2026-4372
Preprint. Discussion started: 11 August 2026

(Kanakidou et al., 2020; Violaki et al., 2018), which may then be hydrolysed via APA in areas where DIP is scarce, such as the Rhodes Gyre.

DOP hydrolysis may be a more continuous mechanism for alleviating phosphorus stress to a small degree, while dust-derived phosphorus acts more sporadically but can drive intense productivity and nitrogen fixation events when it occurs.

Whatever the phosphorus source to stimulate fixation, any new nitrogen introduced through fixation or atmospheric deposition will be quickly incorporated into particulate and dissolved organic matter. Due to its atmospheric origin, this newly formed organic nitrogen would have a low δ^{15}N signature.

Surface waters of the MAW following LIW formation show low δ^{15}N in PN (0.73 ± 0.3‰) but higher values in DON (2.81 ± 0.13‰) (Figure 2j). This suggests that PN better reflects recent nitrogen inputs, possibly due to the labile nature of most PN tightly coupled with phytoplankton biomass, in contrast with the DON pool, which includes a larger refractory fraction (60 - 70% resistant to short-term degradation) with only 30 - 40% in labile or semi-labile form, with residence times of hours, months or years (Aminot and Kérouel, 2004; Doval et al., 1999; Violaki et al., 2010). The PN pool, being more labile (Emeis et al., 2010), likely captures a real-time snapshot of surface production. This may also explain the low PN concentrations, as much may have been consumed, leaving only the more refractory PN with a low δ^{15}N-PN. Thus, Newly Fixed Nitrogen (henceforth NFN) would be expected to appear in the labile fraction of both DON and PN, while the refractory portion of DON retains an older Atlantic-derived signal, explaining the divergence in δ^{15}N between the two pools.

As LIW forms and surface MAW mixes to depth, the DON and PN pools are remineralised, producing nitrate with a δ^{15}N value that reflects a combination of the two sources, explaining why δ^{15}N-NO_3 in newly formed LIW (1.66 ± 0.17‰) lies between δ^{15}N-PN (0.73 ± 0.3‰) and δ^{15}N-DON (2.81 ± 0.13‰). The δ^{15}N of the most labile fractions of DON and PN would not have been measured, as they are rapidly recycled and crucial for phytoplankton nutrition without forming a substantial portion of the standing and measured pool, especially within the DON pool, which is biased toward refractory material. This is a proposed explanation for the stability of the δ^{15}N-DON pool observed in the subtropical oligotrophic North Atlantic (Peng et al., 2018) and may similarly apply to the Rhodes Gyre.

https://doi.org/10.5194/egusphere-2026-4372
Preprint. Discussion started: 11 August 2026

Rapidly recycled nitrogen is likely reflected more in PN, so the δ^{15}N-PN, closer to the low atmospheric δ^{15}N signal, likely has a more substantial influence on the final δ^{15}N-NO_3 in the LIW than δ^{15}N-DON, highlighting an important pathway for NFN to enter the LIW.

The proportion of NFN incorporated into LIW is estimated using the isotopic mass balance in Eq. (1):

$$\delta^{15}N_{measured} = \delta^{15}N_{new} * (X) + \delta^{15}N_{MAW} * (1 - X) \qquad (1)$$

Where: $\delta^{15}N_{measured}$ = δ^{15}N-NO_3 within newly formed outgoing LIW (Figure 4e - green square, 1.66 ± 0.17‰), $\delta^{15}N_{MAW}$ = δ^{15}N-DON of incoming MAW (Figure 4e - green cross, 2.85 ± 0.41‰), $\delta^{15}N_{new}$ = δ^{15}N of NFN (taken as -1‰ to represent the atmospheric source (Carpenter et al., 1997; Minagawa and Wada, 1986)) and x = proportion of NFN being added during LIW formation. This approach can be applied around the LIW formation area, given the defined δ^{15}N within imported and exported water masses (Tuerena et al., 2015). Using this method, we estimate that 31% of the nitrate in the newly formed LIW is newly fixed, equating to 0.72 ± 0.38 µM of new nitrate (out of 2.33 ± 1.03 µM total).

Extrapolating over the full LIW formation volume using a transport volume of 0.7 Sv during its formation (January to March) (Fach et al., 2021; Lascaratos, 1993; Pinardi et al., 2015) or ~5.44×10^{12} m^3 over 90 days, represents 3.92 ± 2.07 Gmol N (or 54.94 ± 29.03 Gg N) of new nitrogen added during formation. The uncertainty of this estimate overlaps with modelled annual nitrogen fixation rates driven by dust deposition across the Mediterranean (70 - 215 Gg N yr^{-1} (Kanakidou et al., 2020)), highlighting the substantial role the Rhodes Gyre may play in regional nitrogen cycling.

This newly fixed nitrogen could be supplied from diazotrophic activity, which requires an adequate phosphorus supply. Diazotrophs in this region are mainly picoplanktonic (< 3 µm) (Bethoux and Copin-Montegut, 1986) and include *Bradyrhizobium*, UCYN-A, *Rhizobium*, γ-proteobacteria and *Crocosphaera watsonii* (UCYN-B) (Rahav et al., 2022; Ridame et al., 2011). Their N:P requirements vary, but to support the 1 µM of NFN between 25 - 62 nM P would be needed, assuming N:P ratios between 40:1 and 16:1. Observed trends in the Rhodes Gyre, declining DOP concentrations (280 ± 62 nM) and increasing DIP

https://doi.org/10.5194/egusphere-2026-4372
Preprint. Discussion started: 11 August 2026

(65 ± 49 nM), alongside estimated APA rates (66.96 - 712.18 nM P d^{-1}), suggest sufficient phosphorus is being supplied to support this nitrogen fixation input.

Scaling the DIP increase to the full LIW formation volume yields an input of 0.35 ± 0.27 Gmol P (10.97 Gg P). This, paired with the newly fixed N, gives an N:P ratio of 15.4 (N* = -0.21 μM), lower than the measured LIW N* of 1.1 μM. To reconcile this, an additional 1.31 Gmol N (18.34 Gg N) must have been added during LIW formation.

Atmospheric nitrogen deposition could account for this shortfall. Modelled deposition over the Rhodes Gyre ranges from 0.02 - 0.20 g N m^{-2} over the LIW formation period (Kanakidou et al., 2020), equating to 0.55 - 5.50 Gg N across the gyre's surface area (27,500 km^2 (Habib et al., 2023)). This is likely an underestimate, however, as atmospheric dissolved nitrogen will be brought in from the surrounding MAW during LIW formation, so including deposition from the broader MAW inflow region (370,000 km^2) increases this estimate to 7.4 - 37.2 Gg N. This is of the same order as the additional 18.34 Gg N required to match the LIW N* of 1.1 μM.

Certain uncertainties and assumptions should be considered when interpreting the results. It is assumed that the calculated NFN concentration is due to fixation (using the atmospheric isotopic signal of -1‰). However, some of this increase may overlap with atmospheric deposition or lateral transport and would be difficult to separate, but the generally lower $\delta^{15}N$ of atmospheric deposition aids in the prediction, being more representative of nitrogen fixation. The increase in DIP across the gyre is assumed to result from the decrease in DOP; this is likely but cannot be confirmed with this dataset. Modelled atmospheric deposition rates are uncertain and variable, as is the area of deposition that contributes to inflow into the gyre. However, the values utilised would provide a reliable deposition estimate within an order of magnitude.

Considering these caveats, this analysis still suggests that nitrogen fixation likely plays a significant role in the Rhodes Gyre and should be considered as a key factor controlling nitrogen dynamics in the newly formed LIW. Atmospheric deposition also contributes notably, although potentially less than fixation in the formation region. Atlantic-derived nitrogen entering with MAW also remains important but is difficult to quantify in surface nutrient dynamics across the Eastern Mediterranean. Multiple nitrogen and phosphorus sources likely contribute to the nitrogen isotope dynamics of LIW formation, with their

https://doi.org/10.5194/egusphere-2026-4372
Preprint. Discussion started: 11 August 2026

relative influence varying seasonally. These observations during the summer stratified period suggest that DOP hydrolysis-driven nitrogen fixation may be a major contributor, supported by changes in DON* and DOP and by high APA rates in the Rhodes Gyre, consistent with mechanisms seen in other ocean regions. Newly fixed or deposited nitrogen enters labile particulate and dissolved organic pools with low $\delta^{15}N$, transferring the isotopic signal to depth as LIW forms during winter convection. These pools are subsequently remineralised within the LIW as it transits through the Mediterranean. Since this study sampled during summer stratification, future research should target winter convection periods to better capture the full extent of nitrogen cycling and the relative roles of fixation and deposition in shaping LIW stoichiometry and $\delta^{15}N$ signatures.

5 Conclusions

As MAW flows from the Western to the Eastern Mediterranean, its nutrient and nitrogen isotope characteristics evolve, reflecting shifting nitrogen and phosphorus sources.

In the west, anthropogenic atmospheric nitrogen deposition dominates, leading to high atmospheric N:P ratios in deposition and maintaining higher N* and low $\delta^{15}N$ values of MAW nitrogen species, with nitrogen fixation providing a smaller contribution. Moving east, the influence of anthropogenic nitrogen declines, along with atmospheric N:P, while dust-derived phosphorus inputs and stimulated nitrogen fixation may play a greater role, particularly in localised areas following dust deposition events. Changing anthropogenic nitrogen additions exert a greater influence on the MAW composition than dust-derived phosphorus, contributing to an overall reduction in N* and $\delta^{15}N$ values in the MAW and shape the nutrient composition of the MAW reaching the LIW formation region in the Rhodes Gyre, a key area for basin-wide Mediterranean biogeochemistry. Here, stimulated nitrogen fixation, particularly through DOP hydrolysis supported by high APA, appears to be a potential mechanism influencing nitrogen dynamics. These processes could explain the observed stoichiometric changes and the estimated input of 0.72 ± 0.38 µM (54.94 ± 29.03 Gg N) of NFN into the LIW during its formation. Atmospheric deposition contributes additional nitrogen (up to 7.4 - 37.2 Gg N per season), suggesting a reduced influence of anthropogenic atmospheric nitrogen deposition vs nitrogen fixation in this region. The NFN and its low

https://doi.org/10.5194/egusphere-2026-4372
Preprint. Discussion started: 11 August 2026

$\delta^{15}N$ signature become incorporated into organic matter, which is remineralised during winter convection and exported to depth with the forming LIW, imprinting its isotopic signal.

These findings highlight the importance of processes occurring in the LIW formation region and the gradient of external inputs to the MAW flowing into it, forming the LIW. These ultimately shape the biogeochemistry of much of the downstream Mediterranean. Understanding the balance of these inputs is crucial for predicting how future changes in nitrogen sources may affect the nutrient transfer to the LIW, internal LIW nutrient cycling and subsequent export to the Atlantic Ocean.

6 Appendices

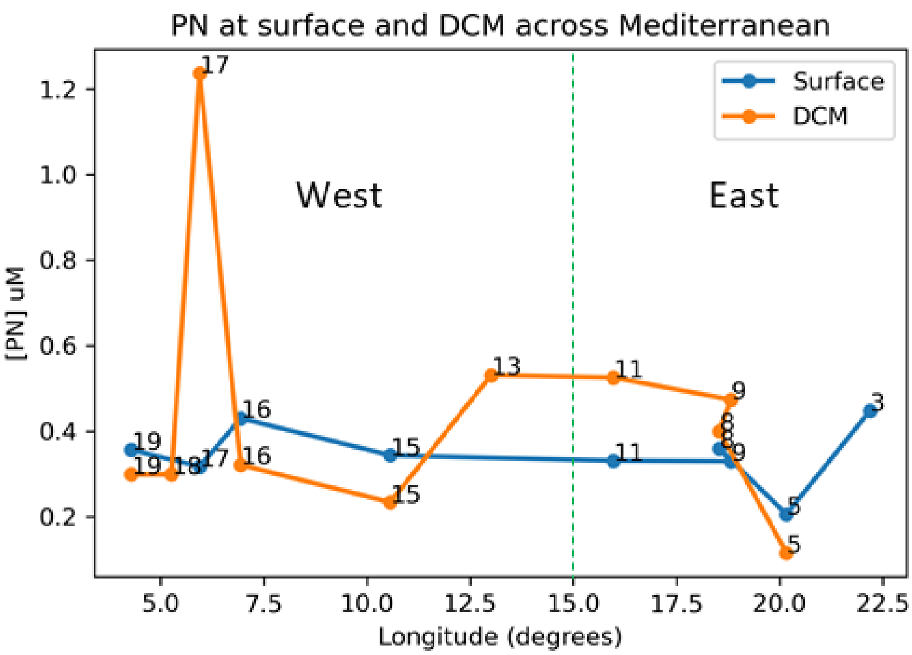

Figure A 1 - PN concentration trends in the surface and DCM within the outgoing MAW. Numbers on each point represent station numbers from the 64PE374 GA04 cruise.

https://doi.org/10.5194/egusphere-2026-4372
Preprint. Discussion started: 11 August 2026

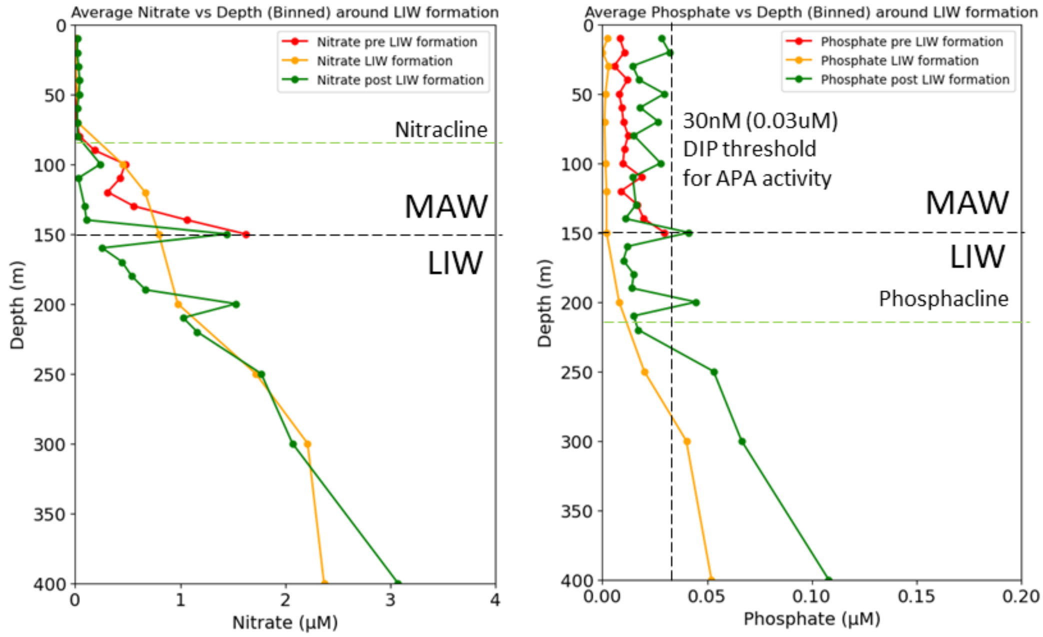

Figure A 2 - Profiles of nitrate and phosphate around the LIW formation area. Average values are calculated between samples in each region outlined in Sect. 2.2 and Figure 4(a) using a consistent 10 m depth bin throughout the profiles.

https://doi.org/10.5194/egusphere-2026-4372
Preprint. Discussion started: 11 August 2026

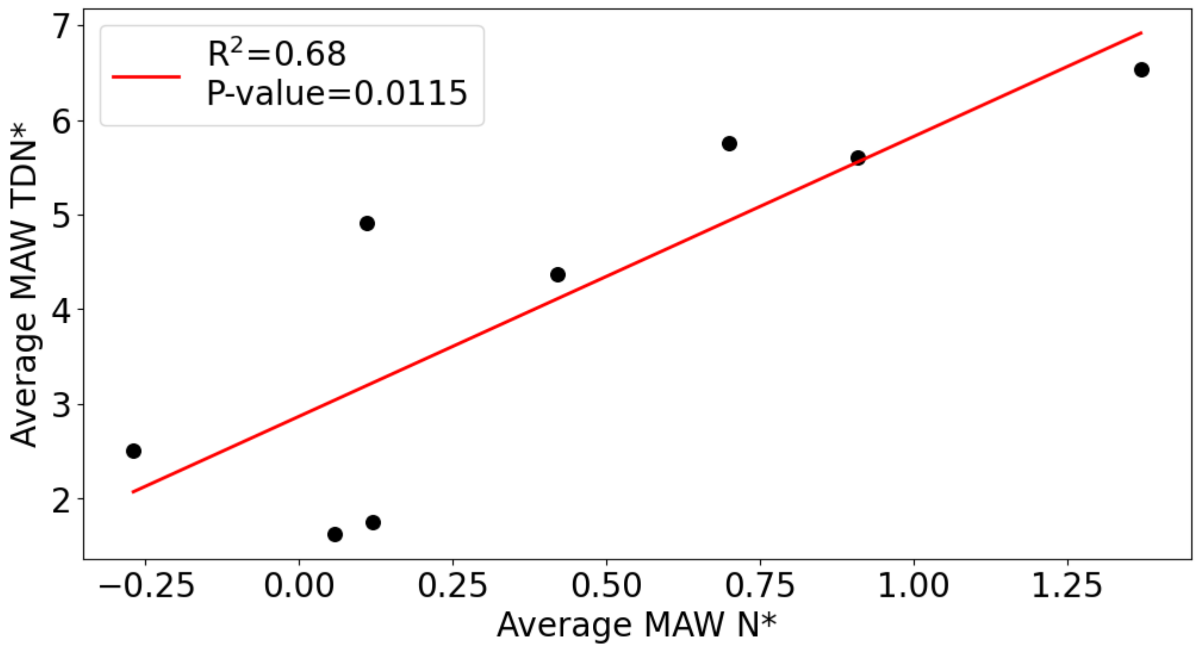

Figure A 3 - Statistically significant correlation ($p<0.05$) between N* and TDN* in the surface MAW water of the Mediterranean. Data is from both the incoming and outgoing MAW water and shows that trends in the N* are related to the overall TDN pool and hence atmospheric inputs described in chapter 3 also correlate with TDN*. Using TDN* rather than N* was considered for comparisons of surface nutrient dynamics to external atmospheric inputs as TDN* may be more representative of surface processes due to including the organic component which is more prevalent in the surface waters. However, a greater coverage of N* data was available than DON* or TDN* (only available for the 374 cruise leg (outgoing MAW) and not for every station, often missing stations with atmospheric deposition fluxes). This correlation shows that the use of the more extensive N* data can be used to approximate the trend in TDN* as well.

https://doi.org/10.5194/egusphere-2026-4372
Preprint. Discussion started: 11 August 2026

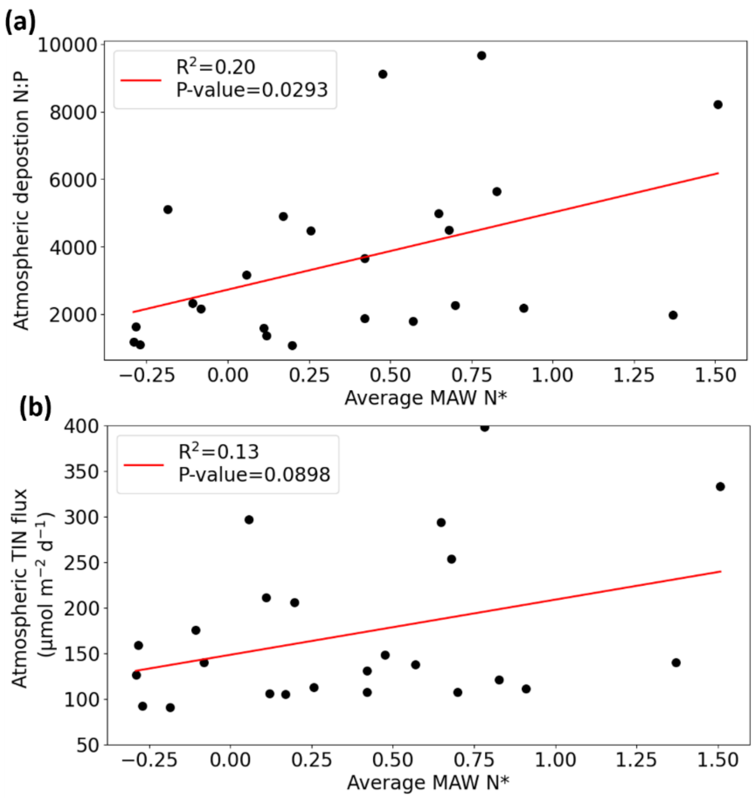

Figure A 4 - The average N* for the whole MAW (incoming and outgoing) vs (a) atmospheric deposition N:P ratio (b) the atmospheric TIN flux.

7 Data availability

Base maps used in figures were from Ocean Data View (Schlitzer, Reiner, Ocean Data View, odv.awi.de, 2025). The nutrient data are available (to view and download) as part of the GEOTRACES Intermediate Data Product (GEOTRACES, 2021) via *doi:10.5285/cf2d9ba9-d51d-3b7c-e053-8486abc0f5fd* which can be accessed online via https://www.egeotraces.org/. The dataset generated from samples analysis for this study is fully available on BODC to download (Francis et al., 2026) via *doi:10.5285/568faca4-3862-53f6-e063-7086abc0ced2*.

https://doi.org/10.5194/egusphere-2026-4372
Preprint. Discussion started: 11 August 2026

8 Author contribution

AF carried out laboratory work to analyse the majority of the samples and wrote the manuscript. RET helped with the study design and manuscript editing. MA analysed nitrate-isotope samples. SR trained AF in the analysis of samples for dissolved organic phosphorus and provided help with interpretations. UB conducted mass spectrometry analysis of TDN/DON isotopes. CM helped with interpretations and helped POC/N analysis at the University of Liverpool. ARB provided the atmospheric deposition dataset and assisted with its interpretation in the context of this manuscript. RSG collected samples during the second leg of the GA04 2013 GEOTRACES GA04 cruise (64PE374). All co-authors provided comments on the manuscript.

9 Competing interests

The authors declare that they have no conflict of interest

10 Acknowledgements

The authors thank the scientists and crew of the 2013 GEOTRACES cruise GA04, particularly Micha Rijkenberg, the cruise leader, and Karel Bakker, for analysing nutrients on board, collecting samples on the first cruise leg (64PE370) and providing the dataset used in this study. The International GEOTRACES Programme is possible in part thanks to the support from the U.S. National Science Foundation (Grant OCE-1840868) to the Scientific Committee on Oceanic Research (SCOR). We also thank Louisa Norman at the University of Liverpool for facilitating the particulate C and nitrogen isotope analysis, and Lukas Marx for his help with the DOP correction process. Data processing was carried out via python and excel. Generative AI (ChatGPT 3.5 and 4.0) was used to assist in debugging Python code written by the primary author for calculations and figure creation. No text, data or interpretations were generated, and the authors reviewed all code modifications.

11 Financial support

NWO (project number: 822.01.015) and Royal NIOZ financed the ship time. AF was funded through the Natural Environment Research Council E4 DTP (grant reference NE/S007407/1) to cover all aspects of project costs including sample collection, analysis and admin. RET and RSG also received funding through this grant for supervision roles.

12 References

Altabet, M. A. and Francois, R.: Sedimentary nitrogen isotopic ratio as a recorder for surface ocean nitrate utilization, Global Biogeochem. Cycles, 8, 103–116, doi:10.1029/93GB03396, 1994.

Aminot, A. and Kérouel, R.: Dissolved organic carbon, nitrogen and phosphorus in the N-E Atlantic and the N-W Mediterranean with particular reference to non-refractory fractions and degradation, Deep Sea Research Part I: Oceanographic Research Papers, 51, 1975–1999, doi:10.1016/J.DSR.2004.07.016, 2004.

Banoub, M. W. and Williams, P. J. le B.: Measurements of microbial activity and organic material in the Western Mediterranean Sea, Deep Sea Research and Oceanographic Abstracts, 19, 433–443, doi:10.1016/0011-7471(72)90053-8, 1972.

Benavides, M., Bonnet, S., Hernández, N., Martínez-Pérez, A. M., Nieto-Cid, M., Álvarez-Salgado, X. A., Baños, I., Montero, M. F., Mazuecos, I. P., Gasol, J. M., Osterholz, H., Dittmar, T., Berman-Frank, I., and Arístegui, J.: Basin-wide N2 fixation in the deep waters of the Mediterranean Sea, Global Biogeochem. Cycles, 30, 952–961, doi:10.1002/2015GB005326, 2016.

Berman-Frank, I. and Rahav, E.: Dinitrogen fixation as a source for new production in the Mediterranean Sea: A review, Nova Science Publishers, Inc., 199–226, 2012.

Bethoux, J. P.: Mean water fluxes across sections in the Mediterranean Sea, evaluated on the basis of water and salt budgets and of observed salinities, Oceanologica Acta, 3, 79–88, 1980.

Bethoux, J. P. and Copin-Montegut, G.: Biological fixation of atmospheric nitrogen in the Mediterranean Sea, Limnol. Oceanogr., 31, 1353–1358, doi:10.4319/lo.1986.31.6.1353, 1986.

https://doi.org/10.5194/egusphere-2026-4372
Preprint. Discussion started: 11 August 2026

Béthoux, J. P., Morin, P., Chaumery, C., Connan, O., Gentili, B., and Ruiz-Pino, D.: Nutrients in the Mediterranean Sea, mass balance and statistical analysis of concentrations with respect to environmental change, Mar. Chem., 63, 155–169, doi:10.1016/S0304-4203(98)00059-0, 1998.

Bonnet, S., Grosso, O., and Moutin, T.: Planktonic dinitrogen fixation along a longitudinal gradient across the Mediterranean Sea during the stratified period (BOUM cruise), Biogeosciences, 8, 2257–2267, doi:10.5194/bg-8-2257-2011, 2011.

Bratek, A., Emeis, K. C., Sanders, T., Wankel, S. D., Struck, U., Möbius, J., and Dähnke, K.: Nitrate sources and the effect of land cover on the isotopic composition of nitrate in the catchment of the Rhône River, Isotopes Environ. Health Stud., 56, 14–35, doi:10.1080/10256016.2020.1723580, 2020.

Carpenter, E. J., Harvey, H. R., Brian, F., and Capone, D. G.: Biogeochemical tracers of the marine cyanobacterium Trichodesmium, Deep Sea Research Part I: Oceanographic Research Papers, 44, 27–38, doi:10.1016/S0967-0637(96)00091-X, 1997.

Casciotti, K. L., Sigman, D. M., Hastings, M. G., Böhlke, J. K., and Hilkert, A.: Measurement of the oxygen isotopic composition of nitrate in seawater and freshwater using the denitrifier method, Anal. Chem., 74, 4905–4912, doi:10.1021/ac020113w, 2002.

Davis, C. E., Blackbird, S., Wolff, G., Woodward, M., and Mahaffey, C.: Seasonal organic matter dynamics in a temperate shelf sea, Prog. Oceanogr., 177, 101925, doi:10.1016/J.POCEAN.2018.02.021, 2019.

Doval, M. D., Pérez, F. F., and Berdalet, E.: Dissolved and particulate organic carbon and nitrogen in the Northwestern Mediterranean, Deep Sea Research Part I: Oceanographic Research Papers, 46, 511–527, doi:10.1016/S0967-0637(98)00072-7, 1999.

Emeis, K. C., Mara, P., Schlarbaum, T., Möbius, J., Dähnke, K., Struck, U., Mihalopoulos, N., and Krom, M.: External N inputs and internal N cycling traced by isotope ratios of nitrate, dissolved reduced nitrogen, and particulate nitrogen in the Eastern Mediterranean Sea, J. Geophys. Res. Biogeosci., 115, 4041, doi:10.1029/2009JG001214, 2010.

Ben Ezra, T., Krom, M. D., Tsemel, A., Berman-Frank, I., Herut, B., Lehahn, Y., Rahav, E., Reich, T., Thingstad, T. F., and Sher, D.: Seasonal nutrient dynamics in the P depleted Eastern Mediterranean Sea,

https://doi.org/10.5194/egusphere-2026-4372
Preprint. Discussion started: 11 August 2026

Deep Sea Research Part I: Oceanographic Research Papers, 176, 103607, doi:10.1016/J.DSR.2021.103607, 2021.

Fach, B. A., Orek, H., Yilmaz, E., Tezcan, D., Salihoglu, I., Salihoglu, B., and Latif, M. A.: Water Mass Variability and Levantine Intermediate Water Formation in the Eastern Mediterranean Between 2015 and 2017, J. Geophys. Res. Oceans, 126, e2020JC016472, doi:10.1029/2020JC016472, 2021.

Fowler, D., Steadman, C. E., Stevenson, D., Coyle, M., Rees, R. M., Skiba, U. M., Sutton, M. A., Cape, J. N., Dore, A. J., Vieno, M., Simpson, D., Zaehle, S., Stocker, B. D., Rinaldi, M., Facchini, M. C., Flechard, C. R., Nemitz, E., Twigg, M., Erisman, J. W., Butterbach-Bahl, K., and Galloway, J. N.: Effects of global change during the 21st century on the nitrogen cycle, Atmos. Chem. Phys, 15, 13849–13893, doi:10.5194/acp-15-13849-2015, 2015.

Francis, A., Tuerena, R. E., Ganeshram, R. S., Ankele, M., Baker, A. R., Dähnke, K., Reynolds, S. E., Baranowski, U., and Mahaffey, C.: Organic nutrients and nitrogen isotopes from GEOTRACES GA04 Mediterranean cruise [Dataset], https://www.bodc.ac.uk/data/published_data_library/catalogue/10.5285/568faca4-3862-53f6-e063-7086abc0ced2/, 2026.

Freyer, H. D.: Seasonal variation of 15N/14N ratios in atmospheric nitrate species, Tellus B: Chemical and Physical Meteorology, 43 B, 30–44, doi:10.3402/TELLUSB.V43I1.15244, 1991.

Garcia, N., Raimbault, P., Gouze, E., and Sandroni, V.: Nitrogen fixation and primary production in Western Mediterranean., C. R. Biol., 329, 742–750, doi:10.1016/J.CRVI.2006.06.006, 2006.

GEOTRACES: GEOTRACES Intermediate Data Product Group (2021). The GEOTRACES Intermediate Data Product 2021 (IDP2021). [Dataset] NERC EDS British Oceanographic Data Centre NOC, doi:doi:10.5285/cf2d9ba9-d51d-3b7c-e053-8486abc0f5fd, 2021.

Gómez, F., González, N., Echevarría, F., and García, C. M.: Distribution and fluxes of dissolved nutrients in the Strait of Gibraltar and its relationships to microphytoplankton biomass, Estuar. Coast. Shelf Sci., 51, 439–449, doi:10.1006/ECSS.2000.0689, 2000.

Grasshoff, K., Kremling, K., and Ehrhardt, M.: Methods of Seawater Analysis, Weinheim, New York, 1983.

https://doi.org/10.5194/egusphere-2026-4372
Preprint. Discussion started: 11 August 2026

Guerzoni, S., Chester, R., Dulac, F., Herut, B., Loÿe-Pilot, M. D., Measures, C., Migon, C., Molinaroli, E., Moulin, C., Rossini, P., Saydam, C., Soudine, A., and Ziveri, P.: The role of atmospheric deposition in the biogeochemistry of the Mediterranean Sea, Prog. Oceanogr., 44, 147–190, doi:10.1016/S0079-6611(99)00024-5, 1999.

Guieu, C., Loÿe-Pilot, M. D., Ridame, C., and Thomas, C.: Chemical characterization of the Saharan dust end-member: Some biogeochemical implications for the Western Mediterranean Sea, Journal of Geophysical Research: Atmospheres, 107, ACH 5-1, doi:10.1029/2001JD000582, 2002.

Habib, J., Ulses, C., Estournel, C., Fakhri, M., Marsaleix, P., Pujo-Pay, M., Fourrier, M., Coppola, L., Mignot, A., Mortier, L., and Conan, P.: Seasonal and interannual variability of the pelagic ecosystem and of the organic carbon budget in the Rhodes Gyre (Eastern Mediterranean): influence of winter mixing, Biogeosciences, 20, 3203–3228, doi:10.5194/BG-20-3203-2023, 2023.

Ibello, V., Cantoni, C., Cozzi, S., and Civitarese, G.: First basin-wide experimental results on N2 fixation in the open Mediterranean Sea, Geophys. Res. Lett., 37, doi:10.1029/2009GL041635, 2010.

Jickells, T. D., Buitenhuis, E., Altieri, K., Baker, A. R., Capone, D., Duce, R. A., Dentener, F., Fennel, K., Kanakidou, M., LaRoche, J., Lee, K., Liss, P., Middelburg, J. J., Moore, J. K., Okin, G., Oschlies, A., Sarin, M., Seitzinger, S., Sharples, J., Singh, A., Suntharalingam, P., Uematsu, M., and Zamora, L. M.: A reevaluation of the magnitude and impacts of anthropogenic atmospheric nitrogen inputs on the ocean, Global Biogeochem. Cycles, 31, 289–305, doi:10.1002/2016GB005586, 2017.

Johannsen, A., Dähnke, K., and Emeis, K.: Isotopic composition of nitrate in five German rivers discharging into the North Sea, Org. Geochem., 39, 1678–1689, doi:10.1016/J.ORGGEOCHEM.2008.03.004, 2008.

Kanakidou, M., Myriokefalitakis, S., Daskalakis, N., Fanourgakis, G., Nenes, A., Baker, A. R., Tsigaridis, K., and Mihalopoulos, N.: Past, Present, and Future Atmospheric Nitrogen Deposition, J. Atmos. Sci., 73, 2039–2047, doi:10.1175/JAS-D-15-0278.1, 2016.

Kanakidou, M., Myriokefalitakis, S., and Tsagkaraki, M.: Atmospheric inputs of nutrients to the Mediterranean Sea, Deep. Sea. Res. 2. Top. Stud. Oceanogr., 171, doi:10.1016/j.dsr2.2019.06.014, 2020.

Knapp, A. N., Sigman, D. M., and Lipschultz, F.: N isotopic composition of dissolved organic nitrogen and nitrate at the Bermuda Atlantic Time-series Study site, Global Biogeochem. Cycles, 19, 1–15, doi:10.1029/2004GB002320, 2005.

Krom, M. D., Kress, N., Brenner, S., and Gordon, L. I.: Phosphorus limitation of primary productivity in the Eastern Mediterranean Sea, Limnol. Oceanogr., 36, 424–432, doi:10.4319/LO.1991.36.3.0424, 1991.

Krom, M. D., Woodward, E. M. S., Herut, B., Kress, N., Carbo, P., Mantoura, R. F. C., Spyres, G., Thingsted, T. F., Wassmann, P., Wexels-Riser, C., Kitidis, V., Law, C., and Zodiatis, G.: Nutrient cycling in the south east Levantine basin of the Eastern Mediterranean: Results from a phosphorus starved system, Deep Sea Research Part II: Topical Studies in Oceanography, 52, 2879–2896, doi:10.1016/J.DSR2.2005.08.009, 2005.

Krom, M. D., Emeis, K. C., and Van Cappellen, P.: Why is the Eastern Mediterranean phosphorus limited?, Prog. Oceanogr., 85, 236–244, doi:10.1016/J.POCEAN.2010.03.003, 2010.

Lascaratos, A.: Estimation of deep and intermediate water mass formation rates in the Mediterranean Sea, Deep Sea Research Part II: Topical Studies in Oceanography, 40, 1327–1332, doi:10.1016/0967-0645(93)90072-U, 1993.

Letscher, R. T. and Moore, J. K.: Preferential remineralization of dissolved organic phosphorus and non-Redfield DOM dynamics in the global ocean: Impacts on marine productivity, nitrogen fixation, and carbon export, Global Biogeochem. Cycles, 29, 325–340, doi:10.1002/2014GB004904, 2015.

Lomas, M. W., Burke, A. L., Lomas, D. A., Bell, D. W., Shen, C., Dyhrman, S. T., and Ammerman, J. W.: Sargasso Sea phosphorus biogeochemistry: an important role for dissolved organic phosphorus (DOP), Biogeosciences, 7, 695–710, doi:10.5194/bg-7-695-2010, 2010.

Longo, A. F., Ingall, E. D., Diaz, J. M., Oakes, M., King, L. E., Nenes, A., Mihalopoulos, N., Violaki, K., Avila, A., Benitez-Nelson, C. R., Brandes, J., McNulty, I., and Vine, D. J.: P-NEXFS analysis of aerosol phosphorus delivered to the Mediterranean Sea, Geophys. Res. Lett., 41, 4043–4049, doi:10.1002/2014GL060555, 2014.

Mahaffey, C., Reynolds, S., Davis, C. E., and Lohan, M. C.: Alkaline phosphatase activity in the subtropical ocean: Insights from nutrient, dust and trace metal addition experiments, Front. Mar. Sci., 1, 122793, doi:10.3389/fmars.2014.00073, 2014.

https://doi.org/10.5194/egusphere-2026-4372
Preprint. Discussion started: 11 August 2026

Mara, P., Mihalopoulos, N., Gogou, A., Daehnke, K., Schlarbaum, T., Emeis, K. C., and Krom, M.: Isotopic composition of nitrate in wet and dry atmospheric deposition on Crete in the Eastern Mediterranean Sea, Global Biogeochem. Cycles, 23, 4002, doi:10.1029/2008GB003395, 2009.

Markaki, Z., Loÿe-Pilot, M. D., Violaki, K., Benyahya, L., and Mihalopoulos, N.: Variability of atmospheric deposition of dissolved nitrogen and phosphorus in the Mediterranean and possible link to the anomalous seawater N/P ratio, Mar. Chem., 120, 187–194, doi:10.1016/J.MARCHEM.2008.10.005, 2010.

Mayer, B., Boyer, E. W., Goodale, C., Jaworski, N. A., Van Breemen, N., Howarth, R. W., Seitzinger, S., Billen, G., Lajtha, K., Nadelhoffer, K., Van Dam, D., Hetling, L. J., Nosal, M., and Paustian, K.: Sources of nitrate in rivers draining sixteen watersheds in the Northeastern U.S.: Isotopic constraints, Biogeochemistry, 57–58, 171–197, doi:10.1023/A:1015744002496, 2002.

McIlvin, M. R. and Casciotti, K. L.: Technical updates to the bacterial method for nitrate isotopic analyses, Anal. Chem., 83, 1850–1856, doi:10.1021/AC1028984, 2011.

Millot, C. and Taupier-Letage, I.: Circulation in the Mediterranean Sea, Life in the Mediterranean Sea: A Look at Habitat Changes, 99–125, doi:10.1007/B107143, 2005.

Minagawa, M. and Wada, E.: Nitrogen isotope ratios of red tide organisms in the East China Sea: A characterization of biological nitrogen fixation, Mar. Chem., 19, 245–259, doi:10.1016/0304-4203(86)90026-5, 1986.

Montoya, J. P.: Nitrogen Stable Isotopes in Marine Environments, Nitrogen in the Marine Environment, 1277–1302, doi:10.1016/B978-0-12-372522-6.00029-3, 2008.

Moutin, T. and Raimbault, P.: Primary production, carbon export and nutrients availability in western and Eastern Mediterranean Sea in early summer 1996 (MINOS cruise), Journal of Marine Systems, 33–34, 273–288, doi:10.1016/S0924-7963(02)00062-3, 2002.

Nehir, M. and Koçak, M.: Atmospheric water-soluble organic nitrogen (WSON) in the eastern Mediterranean: Origin and ramifications regarding marine productivity, Atmos. Chem. Phys., 18, 3603–3618, doi:10.5194/ACP-18-3603-2018, 2018.

Ozsoy, E., Latif, M. A., and Unluata, U.: On the formation of Levantine intermediate water, 1981.

Pantoja, S., Repeta, D. J., Sachs, J. P., and Sigman, D. M.: Stable isotope constraints on the nitrogen cycle of the Mediterranean Sea water column, Deep Sea Research Part I: Oceanographic Research Papers, 49, 1609–1621, doi:10.1016/S0967-0637(02)00066-3, 2002.

Pavlidou, A., Velaoras, D., Karageorgis, A. P., Rousselaki, E., Parinos, C., Dähnke, K., Möbius, J., Meador, T. B., Psarra, S., Frangoulis, C., Souvermezoglou, E., Androni, A., Assimakopoulou, G., Chaikalis, S., Kanellopoulos, T. D., Lagaria, A., Zachioti, P., and Gogou, A.: Seasonal variations of biochemical and optical properties, physical dynamics and N stable isotopic composition in three Northeastern Mediterranean basins (Aegean, Cretan and Ionian Seas), Deep Sea Research Part II: Topical Studies in Oceanography, 171, 104704, doi:10.1016/J.DSR2.2019.104704, 2020.

Peng, X., Fawcett, S. E., van Oostende, N., Wolf, M. J., Marconi, D., Sigman, D. M., and Ward, B. B.: Nitrogen uptake and nitrification in the subarctic North Atlantic Ocean, Limnol. Oceanogr., 63, 1462–1487, doi:10.1002/lno.10784, 2018.

Pinardi, N., Zavatarelli, M., Adani, M., Coppini, G., Fratianni, C., Oddo, P., Simoncelli, S., Tonani, M., Lyubartsev, V., Dobricic, S., and Bonaduce, A.: Mediterranean Sea large-scale low-frequency ocean variability and water mass formation rates from 1987 to 2007: A retrospective analysis, Prog. Oceanogr., 132, 318–332, doi:10.1016/J.POCEAN.2013.11.003, 2015.

Poulos, S. E.: Water Masses of the Mediterranean Sea and Black Sea: An Overview, Water 2023, Vol. 15, Page 3194, 15, 3194, doi:10.3390/W15183194, 2023.

Powley, H. R., Krom, M. D., and Van Cappellen, P.: Understanding the unique biogeochemistry of the Mediterranean Sea: Insights from a coupled phosphorus and nitrogen model, Global Biogeochem. Cycles, 31, 1010–1031, doi:10.1002/2017GB005648, 2017.

Pujo-Pay, M., Conan, P., Oriol, L., Cornet-Barthaux, V., Falco, C., Ghiglione, J. F., Goyet, C., Moutin, T., and Prieur, L.: Integrated survey of elemental stoichiometry (C, N, P) from the Western to Eastern Mediterranean Sea, Biogeosciences, 8, 883–899, doi:10.5194/BG-8-883-2011, 2011.

Putaud, J. P., Raes, F., Van Dingenen, R., Brüggemann, E., Facchini, M. C., Decesari, S., Fuzzi, S., Gehrig, R., Hüglin, C., Laj, P., Lorbeer, G., Maenhaut, W., Mihalopoulos, N., Müller, K., Querol, X., Rodriguez, S., Schneider, J., Spindler, G., Ten Brink, H., Tørseth, K., and Wiedensohler, A.: A European aerosol phenomenology—2: chemical characteristics of particulate matter at kerbside, urban, rural and

https://doi.org/10.5194/egusphere-2026-4372
Preprint. Discussion started: 11 August 2026

background sites in Europe, Atmos. Environ., 38, 2579–2595, doi:10.1016/J.ATMOSENV.2004.01.041, 2004.

Rahav, E., Herut, B., Levi, A., Mulholland, M. R., and Berman-Frank, I.: Springtime contribution of dinitrogen fixation to primary production across the Mediterranean Sea, Ocean Science, 9, 489–498, doi:10.5194/OS-9-489-2013, 2013a.

Rahav, E., Herut, B., Stambler, N., Bar-Zeev, E., Mulholland, M. R., and Berman-Frank, I.: Uncoupling between dinitrogen fixation and primary productivity in the Eastern Mediterranean Sea, J. Geophys. Res. Biogeosci., 118, 195–202, doi:10.1002/JGRG.20023, 2013b.

Rahav, E., Herut, B., Spungin, D., Levi, A., Mulholland, M. R., and Berman-Frank, I.: Heterotrophic bacteria outcompete diazotrophs for orthophosphate in the Mediterranean Sea, Limnol. Oceanogr., 67, 159–171, doi:10.1002/LNO.11983, 2022.

Rees, A. P., Law, C. S., and Woodward, E. M. S.: High rates of nitrogen fixation during an in-situ phosphate release experiment in the Eastern Mediterranean Sea, Geophys. Res. Lett., 33, 10607, doi:10.1029/2006GL025791, 2006.

Ridame, C. and Guieu, C.: Saharan input of phosphate to the oligotrophic water of the open Western Mediterranean Sea, Limnol. Oceanogr., 47, 856–869, doi:10.4319/LO.2002.47.3.0856, 2002.

Ridame, C., Le Moal, M., Guieu, C., Ternon, E., Biegala, I. C., L'Helguen, S., and Pujo-Pay, M.: Nutrient control of N 2 fixation in the oligotrophic Mediterranean Sea and the impact of Saharan dust events, Biogeosciences, 8, 2773–2783, doi:10.5194/BG-8-2773-2011, 2011.

Ridame, C., Dinasquet, J., Hallstrøm, S., Bigeard, E., Riemann, L., Van Wambeke, F., Bressac, M., Pulido-Villena, E., Taillandier, V., Gazeau, F., Tovar-Sanchez, A., Baudoux, A. C., and Guieu, C.: N2 fixation in the Mediterranean Sea related to the composition of the diazotrophic community and impact of dust under present and future environmental conditions, Biogeosciences, 19, 415–435, doi:10.5194/BG-19-415-2022, 2022.

Rijkenberg, M. J. A.: Cruise report 64PE370 on RV Pelagia MedBlack GEOTRACES leg 1, 2013.

Rijkenberg, M. J. A.: Cruise report 64PE374 on RV Pelagia MedBlack GEOTRACES leg 3, 2014.

Sachs, J. P. and Repeta, D. J.: Oligotrophy and nitrogen fixation during Eastern Mediterranean sapropel events, Science, 286, 2485–2488, doi:10.1126/SCIENCE.286.5449.2485, 1999.

Shelley, R. U., Baker, A. R., Thomas, M., and Murphy, S.: Aerosol trace element solubility and deposition fluxes over the Mediterranean Sea and Black Sea basins, Biogeosciences, 22, 585–600, doi:10.5194/BG-22-585-2025, 2025.

Sigman, D. M. and Casciotti, K. L.: Nitrogen Isotopes in the Ocean, Encyclopedia of Ocean Sciences, 1884–1894, doi:10.1006/RWOS.2001.0172, 2001.

Su, B., Song, X., Duhamel, S., Mahaffey, C., Davis, C., Ivančić, I., and Liu, J.: A dataset of global ocean alkaline phosphatase activity, Sci. Data, 10, doi:10.1038/S41597-023-02081-7, 2023.

Thibodeau, B., Miyajima, T., Tayasu, I., Wyatt, A. S. J., Watanabe, A., Morimoto, N., Yoshimizu, C., and Nagata, T.: Heterogeneous dissolved organic nitrogen supply over a coral reef: First evidence from nitrogen stable isotope ratios, Coral Reefs, 32, 1103–1110, doi:10.1007/s00338-013-1070-9, 2013.

Tuerena, R. E., Ganeshram, R. S., Geibert, W., Fallick, A. E., Dougans, J., Tait, A., Henley, S. F., and Woodward, E. M. S.: Nutrient cycling in the Atlantic basin: The evolution of nitrate isotope signatures in water masses, Global Biogeochem. Cycles, 29, 1830–1844, doi:10.1002/2015GB005164, 2015.

Tuerena, R. E., Hopkins, J., Buchanan, P. J., Ganeshram, R. S., Norman, L., von Appen, W. J., Tagliabue, A., Doncila, A., Graeve, M., Ludwichowski, K. U., Dodd, P. A., de la Vega, C., Salter, I., and Mahaffey, C.: An Arctic Strait of Two Halves: The Changing Dynamics of Nutrient Uptake and Limitation Across the Fram Strait, Global Biogeochem. Cycles, 35, e2021GB006961, doi:10.1029/2021GB006961;JOURNAL:JOURNAL:19449224;ISSUE:ISSUE:DOI, 2021.

Varga, G., Újvári, G., and Kovács, J.: Spatiotemporal patterns of Saharan dust outbreaks in the Mediterranean Basin, Aeolian Res., 15, 151–160, doi:10.1016/J.AEOLIA.2014.06.005, 2014.

Violaki, K., Zarbas, P., and Mihalopoulos, N.: Long-term measurements of dissolved organic nitrogen (DON) in atmospheric deposition in the Eastern Mediterranean: Fluxes, origin and biogeochemical implications, Mar. Chem., 120, 179–186, doi:10.1016/J.MARCHEM.2009.08.004, 2010.

Violaki, K., Bourrin, F., Aubert, D., Kouvarakis, G., Delsaut, N., and Mihalopoulos, N.: Organic phosphorus in atmospheric deposition over the Mediterranean Sea: An important missing piece of the phosphorus cycle, Prog. Oceanogr., 163, 50–58, doi:10.1016/J.POCEAN.2017.07.009, 2018.

https://doi.org/10.5194/egusphere-2026-4372
Preprint. Discussion started: 11 August 2026

Wald, T., Fripiat, F., Foreman, A. D., Ryu, Y., Marconi, D., Tanhua, T., Sisma-Ventura, G., Sigman, D. M., Haug, G. H., and Martínez-García, A.: Origins of the Nitrate 15N Depletion in the Mediterranean Sea, Global Biogeochem. Cycles, 39, e2023GB008035, doi:10.1029/2023GB008035, 2025.

Van Wambeke, F., Christaki, U., Giannakourou, A., Moutin, T., and Souvemerzoglou, K.: Longitudinal and vertical trends of bacterial limitation by phosphorus and carbon in the Mediterranean Sea, Microb. Ecol., 43, 119–133, doi:10.1007/S00248-001-0038-4, 2002.

Van Wambeke, F., Taillandier, V., Durrieu de Madron, X., Conan, P., Pujo-Pay, M., Psarra, S., Rabouille, S., Baumas, C., and Pulido-Villena, E.: Mesoscale variability of phosphorus stocks, hydrological and biological processes in the mixed layer in the Eastern Mediterranean Sea in autumn and during an unusually dense winter phytoplankton bloom, Deep Sea Research Part I: Oceanographic Research Papers, 209, 104348, doi:10.1016/J.DSR.2024.104348, 2024a.

Van Wambeke, F., Conan, P., Pujo-Pay, M., Taillandier, V., Crispi, O., Pavlidou, A., Nunige, S., Didry, M., Salmeron, C., and Pulido-Villena, E.: Phosphomonoesterase and phosphodiesterase activities in the Eastern Mediterranean in two contrasting seasonal situations, Biogeosciences, 21, doi:10.5194/bg-21-2621-2024, 2024b.

Weigand, M. A., Foriel, J., Barnett, B., Oleynik, S., and Sigman, D. M.: Updates to instrumentation and protocols for isotopic analysis of nitrate by the denitrifier method, Rapid Communications in Mass Spectrometry, 30, 1365–1383, doi:10.1002/RCM.7570, 2016.